INVESTIGATION OF PROTEIN INTERACTION PARTNERS OF PLANT-SPECIFIC COILED-COIL PROTEINS

A Thesis
by
ALISON RUTH DESHIELDS

Submitted to the Graduate School
at Appalachian State University
in partial fulfillment of the requirements for the degree of
MASTER OF SCIENCE

December 2017
Department of Biology

INVESTIGATION OF PROTEIN INTERACTION PARTNERS OF PLANT-SPECIFIC COILED-COIL PROTEINS

A Thesis
by
ALISON RUTH DESHIELDS
December 2017

APPROVED BY:

Annkatrin Rose, Ph.D.
Chairperson, Thesis Committee

Ece Karatan, Ph.D.
Member, Thesis Committee

Howard S. Neufeld, Ph.D.
Member, Thesis Committee

Zack E. Murrell, Ph.D.
Chairperson, Department of Biology

Max C. Poole, Ph.D.
Dean, Cratis D. Williams School of Graduate Studies

Abstract

INVESTIGATION OF PROTEIN INTERACTION PARTNERS OF
PLANT-SPECIFIC COILED-COIL PROTEINS

Alison R. DeShields
B.S., University of West Florida
M.S., Appalachian State University

Chairperson: Annkatrin Rose, Ph.D.

Arabidopsis thaliana Matrix Attachment Region-Binding Filament-Like Protein 1 (AtMFP1) and Filament-like Protein 4-2 (AtFLIP4-2) are unique chloroplast proteins with a coiled-coil protein motif. Coiled-coil domains act as protein-protein interaction domains; thus, AtMFP1 and AtFLIP4-2 may be involved in protein complex formations. Long coiled-coil protein motifs are more common in eukaryotes than prokaryotes and therefore would not be expected in organelles derived from endosymbiosis. However, AtMFP1 is associated with the thylakoid membrane; and AtFLIP4-2 is thought to be located in the chloroplast envelope and could be involved in vesicle transport to form thylakoids. My goal was to further investigate AtMFP1, AtFLIP4-2, and the proteins that interact with AtMFP1 and AtFLIP4-2, and their direct or indirect involvement in photosynthetic processes.

A large-scale yeast two-hybrid analysis provided candidate interaction partners for the FLIP4 genes in *Arabidopsis thaliana*. A bioinformatics study was performed and provided insight for the AtFLIP4 gene family. To further understand

the roles of the yeast two-hybrid AtFLIP4 interaction partners, selected cDNAs were cloned for future analysis.

Yeast two-hybrid analysis was also used to test the interaction between AtFLIP4-2 and Ran GTPase Activating Protein 1 (AtRanGAP1). AtRanGAP1 has a domain similar to a protein which was found to interact with FLIP4 in tomato. Analysis using the yeast two-hybrid method confirmed interaction of AtFLIP4-2 and RanGAP and also provided evidence that AtFLIP4-2 possesses an activation domain.

Photosynthesis rates, chlorophyll and carotenoid content, and quantum yield measurements in AtMFP1, AtFLIP4-1, and AtFLIP4-2 knock-out mutant plants were observed and compared to wild type plants. Only photosynthesis measurements at a photosynthetic photon flux density of 150 µmol photons m^{-2} s^{-1}, quantum yield, chlorophyll *a* and total chlorophyll content were significantly lower in AtMFP1 knock-out mutant plants.

The Tandem Affinity Purification (TAP) tagging method is an efficient system for identifying *in vivo* protein interaction partners. A TAP tag MFP1/cTAPi vector and a TAP tag FLIP4-2/cTAPi vector were constructed and confirmed. This research provides a means of continued development for the TAP tagging methodology, insight on potential protein interaction partners for AtFLIP4-1 and AtFLIP4-2, and data for future work in understanding the photosynthetic role of AtMFP1.

Acknowledgments

I would like to express my profound appreciation to my committee chair, Professor Annkatrin Rose, who possesses an incredible commitment to and excitement for the research process and who conveyed a level of brilliance through her writing, teaching, and assistantship. Without her guidance and persistent aid this thesis would not have been possible.

I would also like to thank my committee members, Professors Ece Karatan and Howard Neufeld. Professor Karatan's compassion and demand for excellence sets a new standard and I will take her teaching with me in all my future endeavors. Professor Neufeld's dedication to research, teaching, and community outreach is admirable for anyone who loves the environment and botanical ecology. I also appreciate the use of his Portable Photosynthesis Chamber and Alyssa Teat for her guidance through this process.

I would like to thank Dr. Guichuan Hou for allowing me to use the microscope facility and for his software for calculating leaf area. I would like to thank the Appalachian State University Department of Biology for providing funds for my work and the Biology Department members who showed me great love through personal tragedy. I would like to thank Sigma Xi, and the Appalachian State University Office of Student Research for their grants which aided my pursuit for this research and continued effort in the scientific community.

Dedication

"You can give without loving, but you can never love without giving."

-Robert Louis Stevenson

I first dedicate this thesis to my late brother, Brian Howard Steinbeck. Thank you for loving me and giving me a motive for audaciousness.

"The greatness of a community is most accurately measured by the compassionate actions of its members."

-Coretta Scott King

I also dedicate this thesis to my family. Thank you for your love and help. Also, to my community of friends; without you, I would be nothing.

"You may encounter many defeats, but you must not be defeated. In fact, it may be necessary to encounter the defeats, so you can know who you are, what you can rise from, how you can still come out of it."

-Maya Angelou

Lastly, I dedicate this thesis to my best friend, Summer N. Forester. By my side, forever, through all the hurdles, the laughter; you make my life better, you teach me how to be strong and love myself. I would never want to imagine a place without your friendship.

Table of Contents

List of Tables

List of Figures

Introduction

The endosymbiont theory suggests that certain organelles were originally free-living bacteria that were engulfed by another cell as endosymbionts about 2.7 billion years ago (Margulis 1981; Curtis and Clegg 1984; Cavalier-Smith 2000). According to this theory, plastids have evolved from cyanobacteria and formed a symbiotic relationship with their eukaryotic host cells (Curtis and Clegg 1984; Lie and Rose 1992; Cavalier-Smith 2000; Kobyashi et al. 2002). During the evolution of land plants, chloroplast organelles assimilated certain "eukaryotic features" to adjust to their changing environmental conditions present on land (Cavalier-Smith 2000), among which are long coiled-coil proteins. Prokaryotes only have short coiled-coils, so it is unusual to see long coiled-coils in the chloroplasts of plant cells. We hypothesize that they acquired these long coiled-coil proteins from their host eukaryotic cell during the process of endosymbiosis.

The coiled-coil protein fold is simple yet multi-functional and is easily identified by two or more long alpha-helices winding around each other (Odgren et al. 1996; Lupas 1997; Rose et al. 2004; Davis et al. 2009). Coiled-coil proteins consist of two to five amphipathic α-helices that twist around each other to form supercoils (Burkhard et al. 2001; Litowski and Hodges 2001). They are characterized by a heptad repeat with hydrophobic residues in the first and fourth positions and charged polar residues in the fifth and seventh positions (Burkhard et al. 2001). The structure is stabilized by the packing of hydrophobic side chains called "knobs" into

hydrophilic cores called “holes” (Crick 1953). Although all coiled-coils are characterized by the 3, 4 hydrophobic heptad repeat pattern they can also form helical structures with unique oligomerization states (Kammerer 1997). The α-helical coiled-coil structural protein motif facilitates subunit oligomerization of numerous proteins (Fields and Song 1989; Ahlfors et al. 2004).

Coiled-coils are abundant diverse protein motifs that can be involved in transcription regulation, cell growth and proliferation, development of cartilage and bone, and protein-protein interaction (Mason and Arndt 2004; Rose et al. 2005). The primary function of the coiled-coil motif is protein-protein interaction by the oligomerization of individual subunits in a given multimeric protein.

Coiled-coil proteins have long been studied in animals. Keratin, the protein that makes up animal hair, was the first protein to be characterized as a coiled-coil (Crick 1953). Many animal coiled-coil proteins are involved in cytoskeleton formation and movement, such as the muscle protein myosin. By contrast, fewer studies have looked at the function of long coiled-coils in plants. Since less is known about plant coiled-coil proteins and the repeat nature of their sequences causes problems in sequence similarity searches starting with animal coiled-coil sequences, prediction programs were used to identify candidates for further study. These programs aim at predicting if helices will form coiled-coil regions and the oligomeric state. The “ARABI-COIL” database was created as a repository for plant coiled-coil proteins found in the Arabidopsis (*Arabidopsis thaliana*) genome (Rose et al. 2004). In Arabidopsis, 286 proteins are predicted to have long coiled-coil domains. Most of the long coiled-coil proteins investigated in plants have been found to function as

structural proteins involved in nuclear organization, such as lamin-like proteins or nuclear mitotic apparatus proteins (Rose et al. 2004). In addition to these more typical coiled-coil proteins, several chloroplast-localized coiled-coil proteins have also been identified. Chloroplast-localized, long coiled-coil proteins suggest that these proteins could be involved in processes like photosynthesis, light- and stress-responses, or defense mechanisms found only in plants (Rose et al. 2004).

Two eukaryotic-type chloroplast-targeted coiled-coil proteins identified in Arabidopsis, MAR-binding Filament-like Protein 1 (AtMFP1) and Filament-like Protein 4-2 (AtFLIP4-2) may be involved in these features. AtMFP1 contains a long coiled-coil domain spanning the majority of the protein (Gindullis and Meier 1999; Samaniego et al. 2008), while AtFLIP4-2 contains a shorter coiled-coil domain in its C-terminal half. In addition, both proteins are predicted to contain a chloroplast targeting peptide (cTP) and transmembrane domain (TMD). AtMFP1 dual-localizes in the nuclear matrix and chloroplast (Samaniego et al. 2001; Jeong et al. 2003) and has been shown to be an integral membrane protein of the thylakoid membrane with its coiled-coil domain oriented towards the stroma (Jeong et al. 2003). AtFLIP4-2 is targeted to chloroplasts and is predicted to be an integral inner membrane protein of the chloroplast envelope (Richardson 2012). Both of the proteins' functions are unknown; however, due to their coiled-coil protein motif they may be involved in protein complex formation.

One way to better understand the functions of AtMFP1 and AtFLIP4-2 would be to identify their protein-protein interaction partners. Yeast two-hybrid is an appropriate tool to identify hypothetical interaction partners for AtMFP1 and

AtFLIP4-2 *in vitro*. However, a yeast-two hybrid screen performed with tomato MFP1 was only able to identify one interaction partner (MFP1 Attachment Factor 1, MAF1), which is localized at the nuclear pore and not in the chloroplast (Gindullis et al. 1999). Tomato FLIP4 was identified in a yeast two-hybrid screen with MAF1 and found to have two homologs in Arabidopsis, AtFLIP4-1 and AtFLIP4-2. A recent gene duplication event in Arabidopsis has occurred since the divergence of the Brassicaceae family (Barker et al. 2009). This event gave rise to two surviving paralogs, AtFLIP4-1 and AtFLIP4-2 (Reel 2013; Cole 2014). It is hypothesized that AtFLIP4-1 and AtFLIP4-2, in a process of continued evolution, are diverging and specializing in function (Judge 2015). More specifically, these functions may include critical roles such as photosynthesis and drought responses for AtFLIP4-2 and seed set functions for AtFLIP4-1 (Judge 2015). It is unknown whether tomato FLIP4 or AtFLIP4-1 localize to the chloroplast like AtFLIP4-2. A recent large-scale yeast two-hybrid screen in Arabidopsis identified multiple interaction partners for AtFLIP4-1 and AtFLIP4-2, but only a few candidates are predicted to be localized in the chloroplast (Arabidopsis Interactome Mapping Consortium 2011).

One of the challenges after identifying an interaction by yeast two-hybrid analysis is to determine if this interaction happens *in vivo*, and where the interaction is localized. An alternative method to directly identify chloroplast-localized protein complexes would be the Tandem Affinity Purification (TAP) tagging method (*Figure 1.*). TAP tagging takes advantage of the selective binding of a fused affinity tag. Fusion-based affinity protein purification is an excellent method to purify multi-protein complexes and identify them through mass spectrometry (Berggard et al.

2007). A tagged version of the protein is cloned and introduced into the plant cell. Protein complex isolation involves mixing the chloroplast protein extracts with IgG beads, which will attach to a protein A site (ProtA) in the first affinity column (*Figure 1.*). The contaminants are washed out and TEV is added to cleave off the protein of interest with the calmodulin binding domain, plus their unidentified binding protein complexes. Next, the complex is mixed with calmodulin beads and the contaminants are washed out in the second affinity column (*Figure 1.*). Ethylene Glycol-bis-(β-Aminoethyl Ether)-N, N, N', N'- Tetraacetic Acid (EGTA) is then added to bind with calcium releasing the protein of interest and its binding partners from the calmodulin beads. The protein complexes can be separated by SDS-PAGE and the unknown proteins identified through MS analysis. This method has the ability to successfully isolate protein complexes that are associated with the chloroplast envelope membranes (Andrès et al. 2011).

However, TAP-tagging methodology comes with some disadvantages. Protein complexes with more transient affinity have the ability to be lost during the purification steps. Since no complete protocol has been published for the TAP tag isolation of protein complexes from thylakoid membranes, furthering development of a tandem affinity purification protocol is needed.

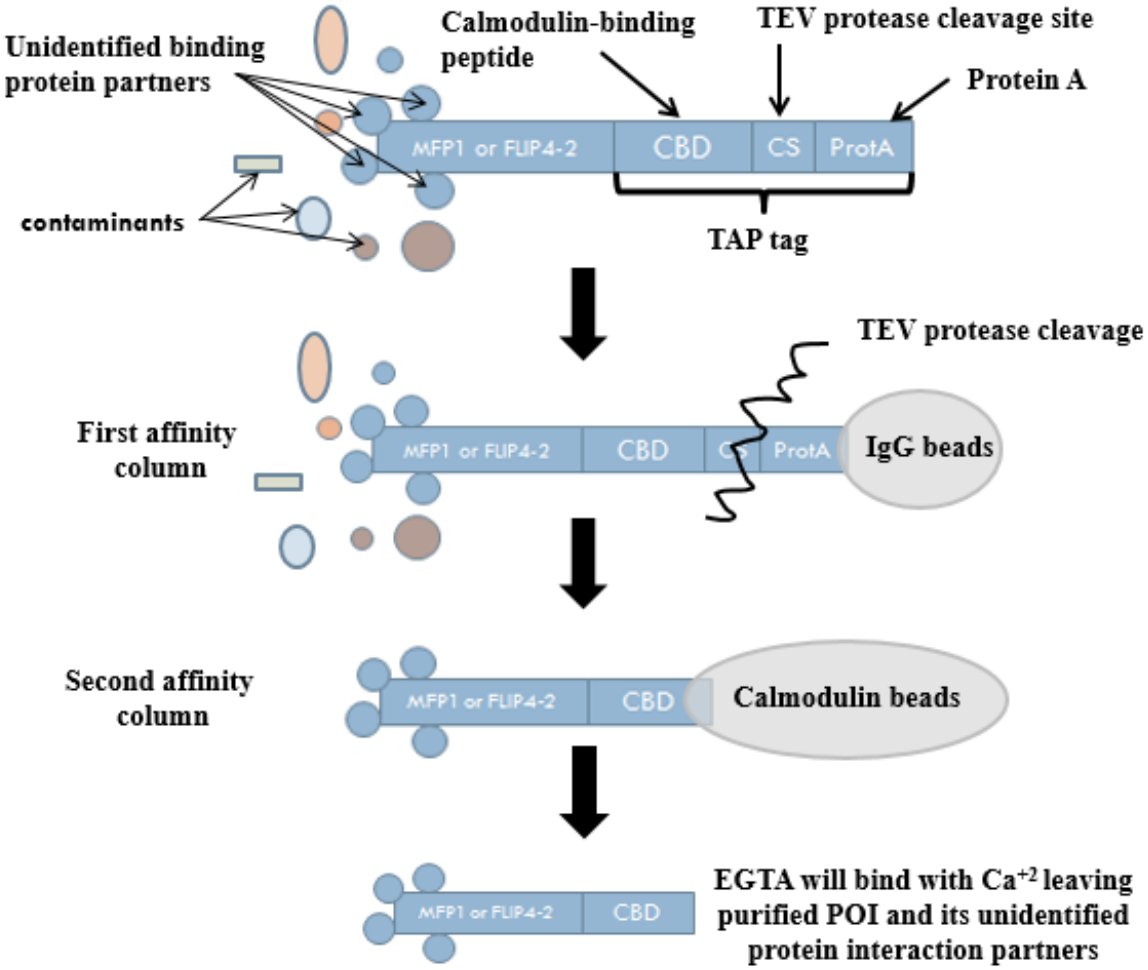

Figure 1. Tandem affinity purification flow chart. Depiction of affinity washes and purification steps to obtain unidentified binding proteins for AtMFP1 or AtFLIP4-2.

Because AtMFP1 and AtFLIP4-2 are localized in the chloroplasts and specific to the land plant lineage, they may be indirectly involved in photosynthesis, which is the primary function of plant chloroplasts. To further understand the possible roles of AtMFP1, AtFLIP4-1 and AtFLIP4-2 in the photosynthetic process, photosynthesis rates, chlorophyll, and carotenoid content measurements in knock-out plants lacking each protein can be compared to wild type Arabidopsis plants. Any differences between mutant and wild type plants would hint at a possible role of membrane-

bound coiled-coil proteins in photosynthesis and provide a better understanding of how land plants evolved.

The objectives of my study were to develop a TAP protocol to identify chloroplast-localized binding partners of AtMFP1 and AtFLIP4-2, to further investigate the putative binding partners identified by yeast two-hybrid analysis, and to determine whether loss of AtMFP1 or AtFLIP4 proteins leads to differences in the efficiency of photosynthesis. My goal was to further characterize these evolutionarily unique proteins, AtMFP1, AtFLIP4-1, and AtFLIP4-2, and how they contribute to the eukaryotic-type features found in chloroplasts of land plants, and their direct or indirect involvement in photosynthetic processes.

Materials and Methods

Plasmid Preparation

The Wizard *Plus*® DNA Purification System (Promega, Madison, WI, USA) was used for isolation of plasmid DNA, and plasmid preparations were performed according to the manufacturer's instructions. For small scale culture (3 mL), the Mini kit was used, while the Maxi kit was used for large scale culture (200 mL). Cultures were incubated in an orbital incubation shaker (VWR, Thorofare, NJ, USA) and centrifuged using a 5415D microcentrifuge (Eppendorf International, Hamburg, DEU) for Mini-preps and a Galaxy 20R centrifuge with swinging bucket rotor (VWR, Bristol, CT, USA) for Maxi-preps. A vacuum manifold (Promega, Vac-Man®, Madison, WI) was used to wash and dry columns. The FastPlasmid™ Mini kit (5PRIME, Gaithersburg, MD, USA) was used according to the manufacturer's instructions to isolate and purify plasmids for sequencing.

DNA Quantification

The ND-1000 spectrophotometer NanoDrop® (Marshall Scientific, Hampton, NH, USA) was used to determine the concentration of DNA in plasmid preparations according to the manufacturer's instructions.

Restriction Digests

NEBcutter V.2.0 (http://nc2.neb.com/NEBcutter2/) was used as a tool to submit a DNA sequence and find a large, non-overlapping open reading frame using the *Escherichia coli* genetic code and the sites for all Type II and commercially available Type III restriction enzymes that cut the sequence. All restriction digests

were performed according to the manufacturer's instructions (New England BioLabs® Inc., NEB, Ipswich, MA, USA). To see small fragments (0.1 – 2.5 kb) in the gel, RNase was added to some restriction digests at a concentration of 1 µg/ml.

Gel Electrophoresis

Agarose gels were prepared by microwaving 1% agarose (agarose from National Diagnostics, Atlanta, GA, USA) in the desired volume of 1 x Tris-Acetate-EDTA (TAE) buffer. Once gels cooled to approximately 50°C, a 1:10,000 dilution of ethidium bromide (EtBr, 10 mg/ml) was added. The solution was then poured into the appropriate sized electrophoresis tray and allowed to solidify. DNA samples were mixed with 6x Loading Buffer (0.25% bromophenol blue, 0.25% xylene cyanol, 15% Ficoll 400) (Thermo Fisher Scientific, Waltham, MA, USA) before loading on the gel. Gels were run in 1x TAE running buffer using the appropriate voltage according to the manufacturer's instructions. Once the gel run was completed, an image was captured using an ImageQuant 300 with IQuant Capture 300 software (American Bioscience, Amersham Place, Buckinghamshire, UK)

Glycerol Stocks

Glycerol stocks were made by combining 1 mL of desired culture and 220 µL of 80% sterile glycerol in a cryogenic screw-cap vial. The vial was then inverted several times to achieve homogeneity, immersed into liquid nitrogen and stored in an 80°C freezer.

Gel Elution

The QIAquick kit (Qiagen, Valencia, CA, USA) was used to perform gel extraction according to the manufacturer's instructions.

Bioinformatics analysis

Bioinformatics databases, programs, and corresponding websites used in this research are presented in Table 1. Vector NTI® Express Designer Software (Thermo Fisher Scientific) was used to analyze sequencing results.

Table 1
Bioinformatics Databases, Their Uses and Websites

Database	Uses	Website
BAR Arabidopsis Interaction Viewer	Construct an interaction map of potential protein partners	http://bar.utoronto.ca/interactions/cgi-bin/arabidopsis_interactions_viewer.cgi
BAR Arabidopsis ePlant	Data visualization tools for multiple levels of plant data	http://bar.utoronto.ca/eplant/
Multicoil	Determines if proteins have a coiled-coil motif	http://cb.csail.mit.edu/cb/multicoil/cgi-bin/multicoil.cgi
ChloroP	Predicts potential binding partners in the chloroplast	http://www.cbs.dtu.dk/services/ChloroP/
TargetP	predicts what plastid the potential binding partner is located	http://www.cbs.dtu.dk/services/TargetP/

Primers

Primer sequences used for PCR and sequencing with melting temperatures (T_m) are presented in Tables 2 and 3. MFP1-TOPO and MFP1-nostop were used to clone AtMFP1 cDNA into pENTR/D-TOPO vector. MFP1-seqF and MFP1-seqR were used in addition to standard primers for sequencing. Promoter Forward, MFP1 Reverse, MFP1 Forward, and Terminator Reverse were used for colony PCR to confirm MFP1/cTAPi, and Promoter Forward, FLIP4-2 Reverse, FLIP4-2 Forward, and Terminator Reverse were used for colony PCR to confirm FLIP4-2/cTAPi.

Table 2
Primer Sequences for AtMFP1 and AtFLIP4-2

Primer	Sequence	T_m
MFP1-TOPO	5’ CACCATGGGTTTCCTGATAGG3’	50.0°C
MFP1-nostop	5’ AGAACTGGTACTGCTCTTTC 3’	56.0°C
MFP1-seqF	5’ CCTGGCATACAGCTAAAGA 3’	58.9°C
MFP1-seqR	5’ GCTTCCTTCCATTCTTCGTG 3’	59.8°C
Promoter Forward	5’ CCTCGGATTCCATTGCCCAGC 3’	60.9°C
MFP1 Reverse	5’ TAACGGAGAAAGTAGTCGGTTTCGC 3’	60.2°C
MFP1 Forward	5’ ACTTCAACGATCACTAGGAGAGGCA 3’	59.3°C
FLIP4-2 Reverse	5’ TGACAGTCAACTATCAAGTAGCGTTCGTAGT 3’	61.2°C
FLIP4-2 Forward	5’ AGAGGCCATAGAGGTGGCAAGGC 3’	63.3°C
Terminator Reverse	5’ CAACCTGCTCGCCGAAGCGA 3’	62.9°C

Table 3
Primer Sequences for cDNA Clones for AtFLIP4 Interaction Partners

Primer	**Sequence**	**Tm**
C62603-for	5’ GATCTCTTAGAAAATTGCCAGTA 3’	57.6°C
C62603-rev	5’ TCTCGTCTTTGAACCAGTTAAG 3’	57.6°C
U17386-for	5’ CACGCGTTCTTAGTCGGTA 3’	57.5°C
U17386-rev	5’ CTTAGAAGCAACAGATTGTGG 3’	57.5°C
U22824-for	5’ CACAAGGGAGGTGAAAGTA 3’	56.4°C
U22824-rev	5’ AGCCGATCCAGAAGAAACAG 3’	56.4°C
U11815-for	5’ CGTAGTGACTTCGTCGGTA 3’	57.5°C
U11815-rev	5’ CACATGCGCTAACAACTTTAA 3’	57.5°C
U21287-for	5’ CTCTCGACGCCAACGGTA 3’	58.4°C
U21287-rev	5’ CCTTAAGCATAGAGACACCAA 3’	58.4°C
U13452-for	5’ TCTACATTGATTCTTAGCGGTA 3’	56.4°C
U13452-rev	5’ ATCACTGGCCTGTGTG 3’	56.4°C
U68501-for	5’ GGAGCAATGCACAGGGTA 3’	59.5°C
U68501-rev	5’ CGCTCTGTCACTTCCCC 3’	57.3°C
U68182-for	5’ TCTACCTCTCTGAACGGTA 3’	55.0°C
U68182-rev	5’ TGAAGGCTTGTTTTTGCC 3’	56.4°C
U12352-for	5’ TCAAGGAGCATCGAAGGTA 3’	55.4°C
U12352-rev	5’ TAATACAAGAAACCAATATCTCC 3’	55.5°C
U11195-for	5’ TCAAGGAGCATCGAAGGTA 3’	55.0 °C
U11195-rev	5’ TAATAGAAGAAACCAATATCTCC 3’	56.3°C
U10308-for	5’ TCCTTCGACGTAGCGGTA 3’	56.3°C
U10308-rev	5’ TGAGGTGCTATTGACATAGAA 3’	55.4°C

PCR reactions were performed using Taq polymerase (GenScript®, Grand Cayman, KY) according to the manufacturer’s recommendations. Template amounts

used were 0.5 µl of plasmid prep for cDNA amplification or a single colony resuspended in the reaction for colony PCR. PCR program settings used for amplification of AtMFP1 cDNA, colony PCR, and AtFLIP4 cDNA clones are presented in Tables 4, 5, and 6.

Table 4
PCR Settings for AtMFP1 Cloning

PCR Settings	Temperature (°C)	Time (sec.)
Pre-denaturation	95	120
Denaturation	95	30
Annealing	50	45
Extension	72	60
Extension	72	420
Number of Cycles	5	na
Denaturation	95	30
Annealing	55	45
Extension	72	60
Extension	72	420
Number of Cycles	25	na
Final Extension	72	180

Table 5
PCR Settings for cDNA Clones of AtFLIP4 Interaction Partners

PCR Settings	Temperature (°C)	Time (sec.)
Pre-denaturation	95	120
Denaturation	95	20
Annealing	50	20
Extension	72	30
Number of Cycles	30	na
Final Extension	72	180

Table 6
Settings for Colony PCR

PCR Settings	Temperature (°C)	Time (sec.)
Pre-denaturation	95	300
Denaturation	95	60
Annealing	60	60
Extension	72	60
Number of Cycles	1	na
Final Extension	72	300

Gateway ENTR Vector Cloning

AtMFP1 cloning.

To clone TAP-tagged AtMFP1, the AtMFP1 cDNA, lacking the stop codon, was first amplified by PCR (Tables 2 and 5), cloned into the TOPO-ENTR vector (Thermo Fisher Scientific) and transformed into One Shot™ TOP 10 chemically competent cells (Thermo Fisher Scientific) according to the manufacturer's instructions. Positive clones were selected by restriction digest and confirmed through sequencing (Retrogen, San Diego, CA, USA).

Cloning of the potential AtFLIP4 binding partners.

cDNAs for the potential binding partners for AtFLIP4-1 and AtFLIP4-2 (Table 12) were amplified by PCR (Tables 3 and 4), cloned into the TOPO-ENTR vector, and transformed into OneShot Top 10 chemically competent cells (Thermo Fisher Scientific) according to the manufacturer's instructions. Positive clones were selected by restriction digest and confirmed through sequencing (Retrogen).

Amplification of DEST Vectors

To amplify destination vectors containing the *ccdB* negative selection marker, DB3.1™ chemically competent cells were transformed with 0.5 µl of plasmid DNA (cTAPi, pDEST™ 22, or pDEST™ 32) according to the manufacturer's instructions (Thermo Fisher Scientific). Transformed cells were streaked onto YEP medium (10 g Peptone (Sigma-Aldrich, St. Louis, MO, USA), 10 g yeast extract powder (USB Corporation, Cleveland, OH, USA), 5 g sodium chloride (USB), 15 g agar (IBI Scientific, Peosta, Iowa, USA) for plates) with the appropriate antibiotics

(spectinomycin (100 mg/ml) for cTAPi, ampicillin (100 mg/ml) for pDEST22, and gentamycin (100 mg/ml, Sigma-Aldrich) for pDEST 32).

Gateway LR Reactions

LR reaction for cTAPi vector.

To create the plasmids MFP1/cTAPi and FLIP4-2, cTAPi, Gateway LR Clonase™ II enzyme mix (Thermo Fisher Scientific) was used to catalyze recombinations of MFP1/ENTR and FLIP4-2/ENTR with the cTAPi destination vector (*Figure 2.*) according to the manufacturer's instructions. The cTAPi vector was generously donated from the Fromm lab (Rohila et al. 2004) to generate the expression clones MFP1/cTAPi and FLIP4-2/cTAPi (*Figure 7.* B and C). AtFLIP4-2/ENTR had already been cloned previously in the Rose lab.

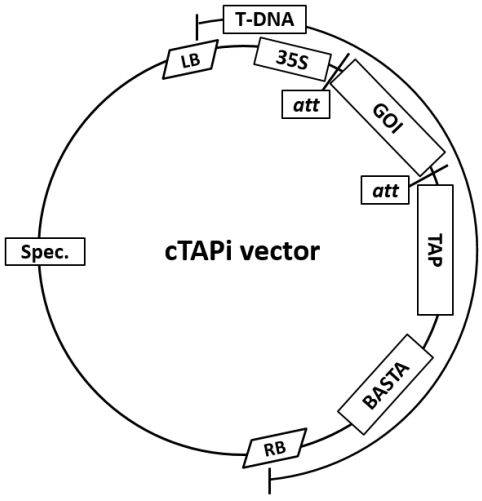

Figure 2. Plasmid map of cTAPi vector. LB, RB, left and right borders of the T-DNA; 35S, plant-specific promoter (CaMV 35S) *att* sites flanking the gene of interest (GOI; AtMFP1 or AtFLIP4-2 cDNA); Spec., spectinomycin resistance gene for selection in bacteria; TAP, Tandem Affinity Purification-tag sequence; BASTA, herbicide resistance gene for selection in plants. The half circle represents the T-DNA which was inserted into the plant genome.

LR reaction for yeast two-hybrid clones.

To create GUS control plasmids for yeast two-hybrid analysis, Gateway LR Clonase™ II enzyme mix was used according to the manufacturer's instructions to catalyze recombination of pENTR™ - gus into pDEST™ 22 and pDEST™ 32 to generate the expression clones GUS/pDEST22 and GUS/pDEST32 (*Figure 13.* B and C). All three plasmids were acquired from Thermo Fisher Scientific.

Transformation of *Agrobacterium*

Preparation of competent cells.

A small overnight culture of *Agrobacterium tumefaciens* GV3101 (cells generously donated by the Meier lab at the Ohio State University) was grown in YEP medium with 50 µg/ml gentamycin (Sigma-Aldrich) and 10 µg/ml rifampicin (Sigma-Aldrich) overnight at 28°C in an incubator shaker. One mL of the overnight culture was added to 400 mL of YEP and grown for 8 hours at 28°C in a shaking incubator. The optical density of the sample was measured in a Genesys 20 spectrophotometer (Thermo Fisher Scientific) at a wavelength of 600 nm. At an OD_{600} of 1.096, the 400 mL culture was split into two and placed into a pre-chilled 4°C centrifuge for 10 minutes at 5,000 rpm. The supernatant was discarded and a wash step was performed by adding 2 mL of sterile cold deionized water to the culture, centrifuging the culture at 5,000 rpm at 4°C and removing the supernatant. Four additional wash steps were performed and the cells were then re-suspended in 10% glycerol. To calculate cell density, an iN CYTO C-Chip disposable hemocytometer (VWR, Radnor, PA, USA) was used. The cells were counted under a microscope with the aid of the

hemocytometer and determined to be at a density of 5 x 10^7 cells/mL. Cells were aliquoted, frozen in liquid nitrogen, and stored at -80°C until later use.

Electroporation.

Forty microliters of competent *Agrobacterium tumefaciens* GV3101 cells were combined with 2 ng of desired plasmid in a pre-chilled 1mm gap electroporation cuvette (Eppendorf AG, Hamburg, DEU). The cuvette was then placed into a Multiporator® (Eppendorf, Hauppauge, NY, USA) with the mode set to prokaryotes 'O', voltage 1800V, and a time constant of 5 milliseconds. One mL of BD Difco™ Super Optimal Broth (SOC) media (Thermo Fisher Scientific) was added to the cuvette and the mixture was transferred into a microcentrifuge vial and allowed to incubate at 28°C for 1 hour and 45 minutes with constant shaking. The cultures were centrifuges and the supernatant except for 100 µl was removed. The cultures were resuspended and 100 µL were then plated on YEP with antibiotics added for selection: 10 µl/ml of rifampicin (Sigma-Aldrich), 25 µl/ml of gentamycin (Sigma-Aldrich), 100 µl/ml spectinomycin (Sigma-Aldrich), and 30 µl/ml streptomycin (Sigma-Aldrich). The plates were allowed to incubate at 28°C for approximately three days. After incubation, colony PCR was performed to verify transformation success and glycerol stocks were made with the positive colonies and stored at -80°C.

Yeast two-hybrid Analysis

Two types of yeast strains, YRG-2 (Clontech, Mountain View, CA, USA) and PJ69-4A (James et al. 1996) were used. Competent yeast cells were previously prepared in the Rose lab and frozen at -80°C. Two µg of DNA constructs and 50 µg fish sperm DNA (Thermo Fisher Scientific) were mixed together and added to frozen

competent cells. The mixture was allowed to thaw at 37°C for 5 minutes while shaking. One mL of solution B (200 mM BICINE, pH 8.35-adjusted with KOH, 40% PEG 1000, filter sterilized and stored at -20°C) was added and gently mixed. The cells were allowed to incubate at 30°C for 60 minutes with no shaking. After 60 minutes, the cells were centrifuged at 3,000 rpm at room temperature and the supernatant was discarded. The cells were washed with 100 µL of solution C (10 mM BICINE, pH 8.35-adjusted with KOH, 140 mM NaCl, filter sterilized) and incubated at room temperature. The cells were spun again; supernatant was discarded, and re-suspended in 100 µL of solution C. All constructs were then plated on synthetic dropout (SD) medium with no leucine or tryptophan (6.7 g yeast nitrogen base without amino acids, pH 5.8, and 20 g agar in 850 ml H_2O, autoclaved, and allowed to cool to 55°C, 50 mL of 40% glucose solution and 100 mL of 10x -Leu/-Trp dropout solution was added after autoclaving before pouring plates). The plates were then incubated at 30°C for 5 days. To test for interaction, colonies of transformed yeast were streaked on SD with no leucine, tryptophan, or histidine.

Photosynthesis measurements

Seeds for wild type (WT) Arabidopsis Wassilewskija (WS) ecotype, WT Columbia (Col.) ecotype, the T-DNA line SALK_074693, which carries an exon insertion in AtFLIP4-1, and the T-DNA line SALK_033887, which carries an exon insertion in AtFLIP4-2, were acquired from the Arabidopsis Biological Resource Center (ABRC, Columbus, OH, USA). Seeds were planted on Burpee 16XL Super Growing Pellets (Burpee, Warminster, PA, USA), subjected to cold treatment (2-3 days at 4°C) and transferred to a Percival Environmental Chamber E-30B on long day

settings: light 6:00 am – 10 pm at 23°C and dark 10 pm – 6 am at 20°C using white light at 111 µmol/m^2/sec (Percival Scientific, Perry, IA, USA). Four plants of each genotype, T-DNA knock-out mutant K-8-5, which cannot produce AtMFP1 (Jeong et al. 2003), and the corresponding wild type (WS) plants, were moved into model SC-7 Ray Leach Cone-tainers (Stuewe and Sons Inc., Tangent, OR, USA) after 20 days and put back in the growth chamber overnight to equilibrate. To compare the AtFLIP4 mutants and the corresponding wild type (Col.), eight plants of each genotype were moved into Cone-tainers after 70 days and put back in the growth chamber overnight to equilibrate.

Each plant used for analysis was set up according to the Whole-Plant Arabidopsis Chamber instruction manual. Eberhard Faber modelling clay was place around the soil of each plant to minimize effects of soil gas exchange on plant exchange rates. Total leaf area was determined by analyzing a photo of each plant with the Microsuite™ Five image software (Olympus, Center Valley, PA, USA) and calibrating the photo by using a 10 mm section of a ruler in the photo. The Whole-Plant Arabidopsis Chamber 6400-17 with RGB light source was attached to the LiCor LI-6400XT Portable Photosynthesis System (LiCor Biosciences, Lincoln, NE, USA). Conditions were set to match those in the growth chamber ($[CO_2]$ = 400 ppm, RH = 35-50%, temperature = 23°C). Photosynthesis-irradiance curves were recorded for three biological replicates based on CO_2 uptake per time and leaf area as photosynthetic photon flux density (PPFD) was decreased stepwise before increasing up to 75% of full sunlight (150, 125, 100, 75, 50, 25, 0, 150, 300, 500, 750, 1000, 1250, 1500 µmol m^{-2} s^{-1}). This experiment was conducted to test whether the two

genotypes responded differently at low vs high irradiances. All data from the Li-6400XT were uploaded and analyzed by the LandFlux.org software (LightResponseCurveFitting 1.0).

Chlorophyll/Carotenoid measurements

To determine the chlorophyll content, all leaves from each plant were pooled and 3 mL of N, N,-dimethylformamide were dispensed into each tube and incubated in the dark for 24 hours. After the 24-hour extraction period, the leaf samples were removed and the extract put into a quartz cuvette to measure absorption at 420 nm using a Genesys20 spectrophotometer (Thermo Fisher Scientific). If absorption was above 0.9 the sample was diluted and the dilutions were used to calculate the final chlorophyll content. The instrument was zeroed at 720 nm with a DMF blank and the absorbance of each sample was measured at 470 nm, 647 nm and 664 nm. The following equations were used to calculate the pigment concentrations of each sample:

Chlorophyll *a* = $12.00*A_{664} - 3.11*A_{647}$

Chlorophyll *b* = $-4.88*A_{664} - 20.78*A_{647}$

Chlorophyll Total = $7.12*A_{664} - 17.67*A_{647}$

Carotenoids = $(91000*A_{470} - 2.05*C_a - 114.8*C_b)/245$

where:

A_{470}, A_{647}, and A_{664} are the absorbance at 470, 647, and 664 nm, respectively.

C_a is chlorophyll *a* concentration in mg/mL; C_b is chlorophyll *b* concentration in mg/mL; Carotenoids is the carotenoid concentration in mg/mL

The final values for pigment content for the leaves were expressed as mg pigment/cm^2 of leaf. Subsequent statistical analyses (t-tests to compare genotypes) were done using SigmaPlot 12.5 (Systat Software, San Jose, CA, USA).

Results

Cloning of AtMFP1 and AtFLIP4-2 TAP constructs

The plasmids MFP1/cTAPi and FLIP4-2/cTAPi were cloned to be used in tandem affinity purification of chloroplast protein complexes. The first step in acquiring the plasmid vectors MFP1/cTAPi and FLIP4-2/cTAPi was to design primers to use for PCR and sequencing (Table 2). The cTAPi vector was confirmed by a Mini prep, restriction digest, and gel electrophoresis (*Figure 3.*). As expected, based on the vector sequence, the plasmid was digested into 3.8 and 8.5 kb fragments by EcoRI and 1.1, 2.5, and 8.6 kb fragments by PstI. The AtMFP1 cDNA was amplified with PCR and confirmed through gel electrophoresis by showing the size of the amplified AtMFP1 cDNA band as 2.3 kb (*Figure 4.*). The amplified AtMFP1 cDNA PCR product was cloned into TOPO-ENTR to form the MFP1/pENTR vector. Clones with correctly inserted AtMFP1 cDNA were selected through restriction digest and gel electrophoresis (*Figure 5.*). Clones 2, 5, and 8-12 showed the band pattern corresponding to the correctly inserted AtMFP1 cDNA (*Figure 6.*). Clones 9-12 were selected for sequencing and a Mini prep, restriction digest and gel electrophoresis were performed (data not shown). Clone 11 showed no PCR errors in the sequence and was selected for continued work (*Figure 7.*). AtFLIP4-2/pENTR plasmid vector was already acquired previously in the Rose lab.

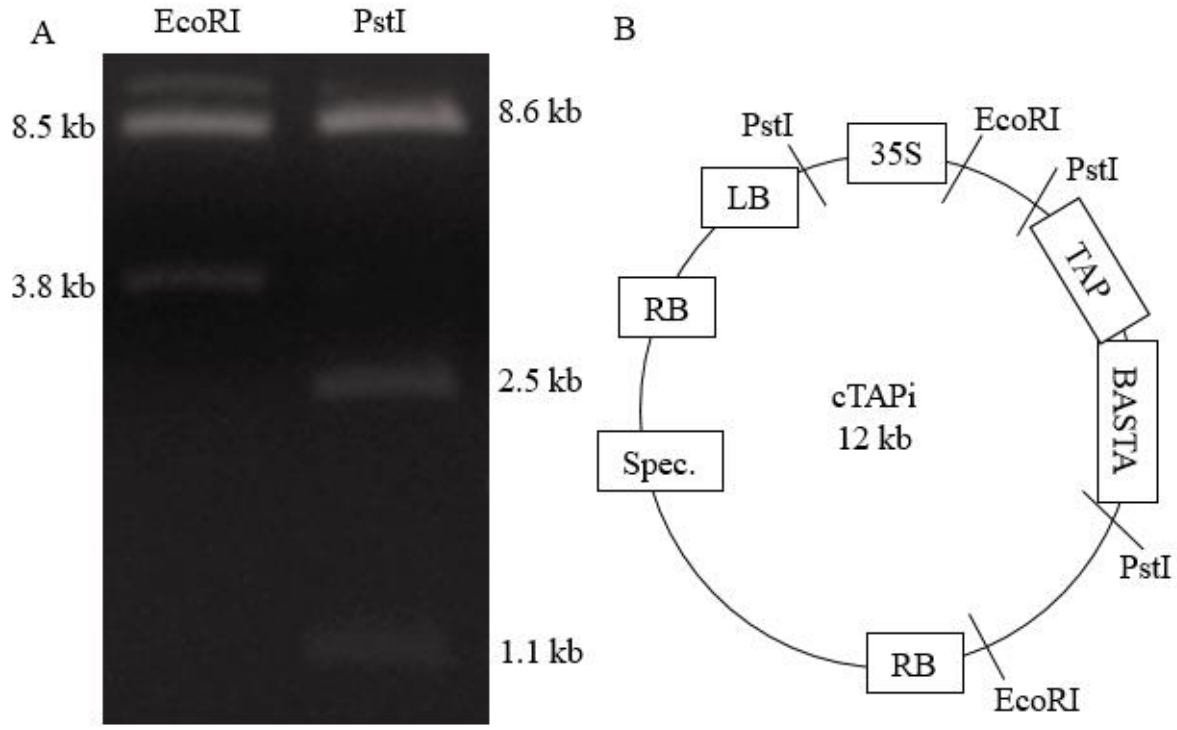

*Figure 3***.** Confirmation of cTAPi vector. A, Restriction digest with enzymes EcoRI and PstI confirming the cTAPi DNA plasmid vector. EcoRI restriction enzyme cuts the DNA at 8.5 kb and 3.8 kb. PstI restriction enzyme cuts the DNA at 8.6 kb, 2.5 kb, and 1.1 kb. B, vector map showing the location of restriction sites.

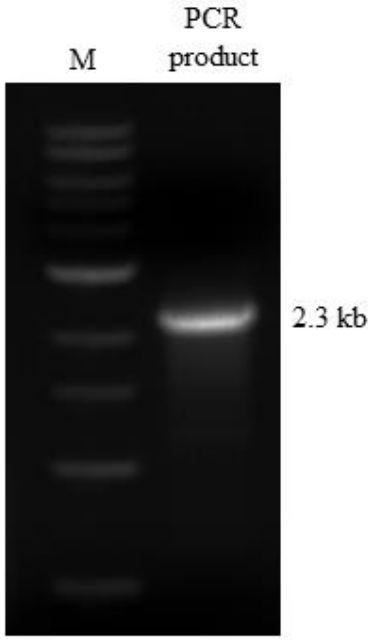

Figure 4. Confirmation of AtMFP1 cDNA PCR product. The 1kb DNA Ladder (NEB) was used as marker (M) to identify the size of the AtMFP1 cDNA PCR product band, which had the expected size at 2.3 kb.

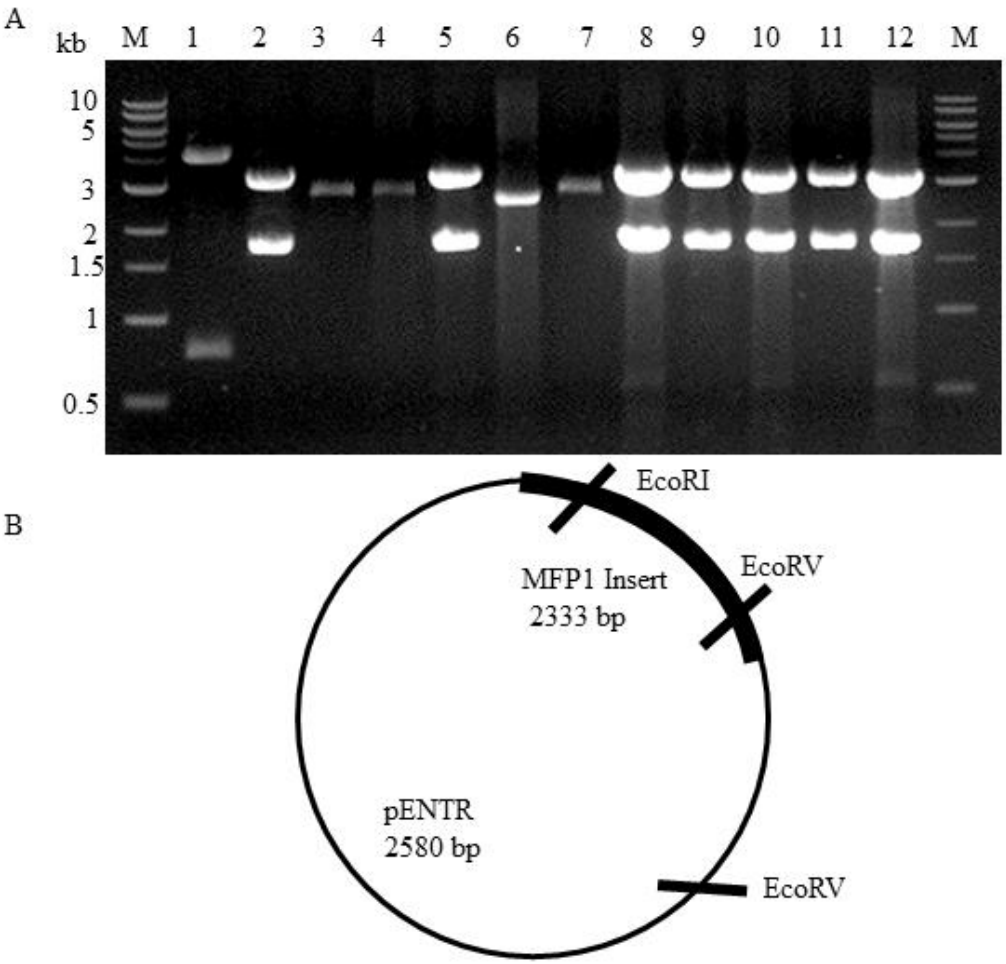

Figure 5. MFP1/pENTR vector confirmation. A, Restriction enzymes EcoRI and EcoRV were used to verify the AtMFP1 cDNA was inserted into pENTR vector correctly. Lane 1 depicts AtMFP1 inserted into pENTR vector the wrong way (1145 bp and 3768 bp). Lanes 3, 4, 6 and 7 depict AtMFP1 not inserted into pENTR vector (2580 bp). Lanes 2, 5, and 8-12 verify that AtMFP1 was inserted into the pENTR vector correctly (1834 bp), M = marker (1 kb DNA Ladder). B, vector map showing the location of the restriction sites.

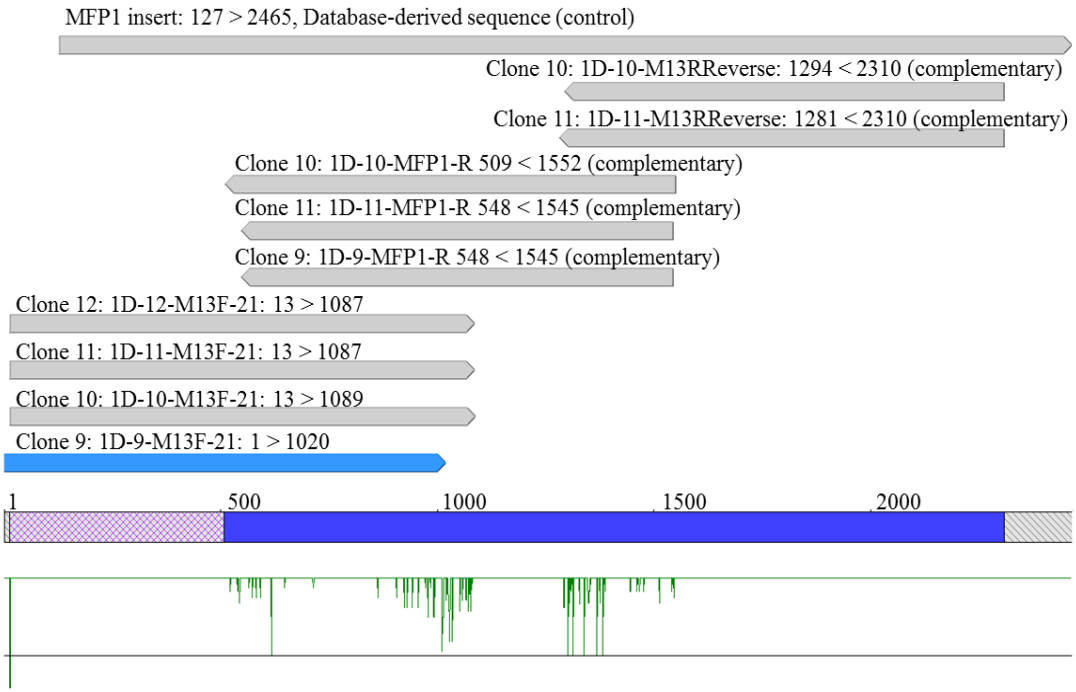

Figure 6. AtMFP1 insert sequencing contig in Vector NTI. Clone 11 showed perfect sequence matching AtMFP1 (excluding stop codon) in the database control and was selected for continued work.

Once MFP1/pENTR vector was confirmed, the LR Clonase reaction was used to combine AtMFP1 and AtFLIP4-2 into the cTAPi destination vector using the Gateway cloning system. A Mini prep, restriction digest, and gel electrophoresis confirmed the MFP1/cTAPi and FLIP4-2/cTAPi plasmid vectors (*Figure 7.*). Maxi preps of clone 1 for MFP1/cTAPi and clone 1 for FLIP4-2/cTAPi plasmid vectors were performed and confirmed by a restriction digest and gel electrophoresis (data not shown).

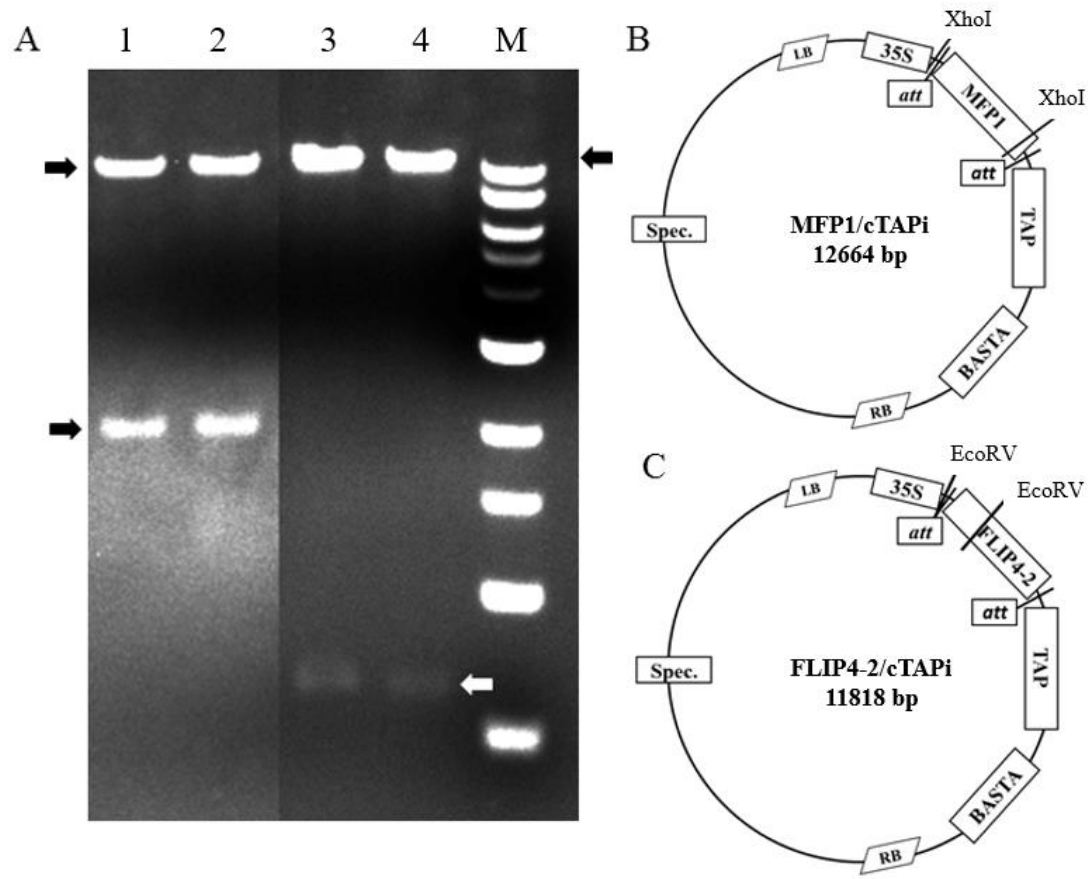

Figure 7. Confirmation of MFP1/cTAPi and FLIP4-2/cTAPi. A, Lane 1 and 2 represents the restriction enzyme digest confirmation of MFP/cTAPi with XhoI and lane 3 and 4 represents the restriction enzyme digest confirmation of FLIP4-2/cTAPi with EcoRV. M is the 1 kb marker. B, restriction map of MFP1/cTAPi. C, restriction map of FLIP4-2/cTAPi.

MFP1/cTAPi and FLIP4-2/cTAPi plasmid vectors were transformed into electrocompetent *A. tumefaciens* GV3101. Once MFP1/cTAPi and FLIP4-2/ cTAPi were mixed with the *A. tumefaciens* GV3101 the electroporation steps were performed to allow the cellular introduction of the plasmid. After electroporation and growing the colonies on selection plates, colony PCR was performed with primers for MFP1/cTAPi or FLIP4-2/cTAPi (Table 6 and *Figure 8*). Successful transformation into Agrobacterium was confirmed for both constructs.

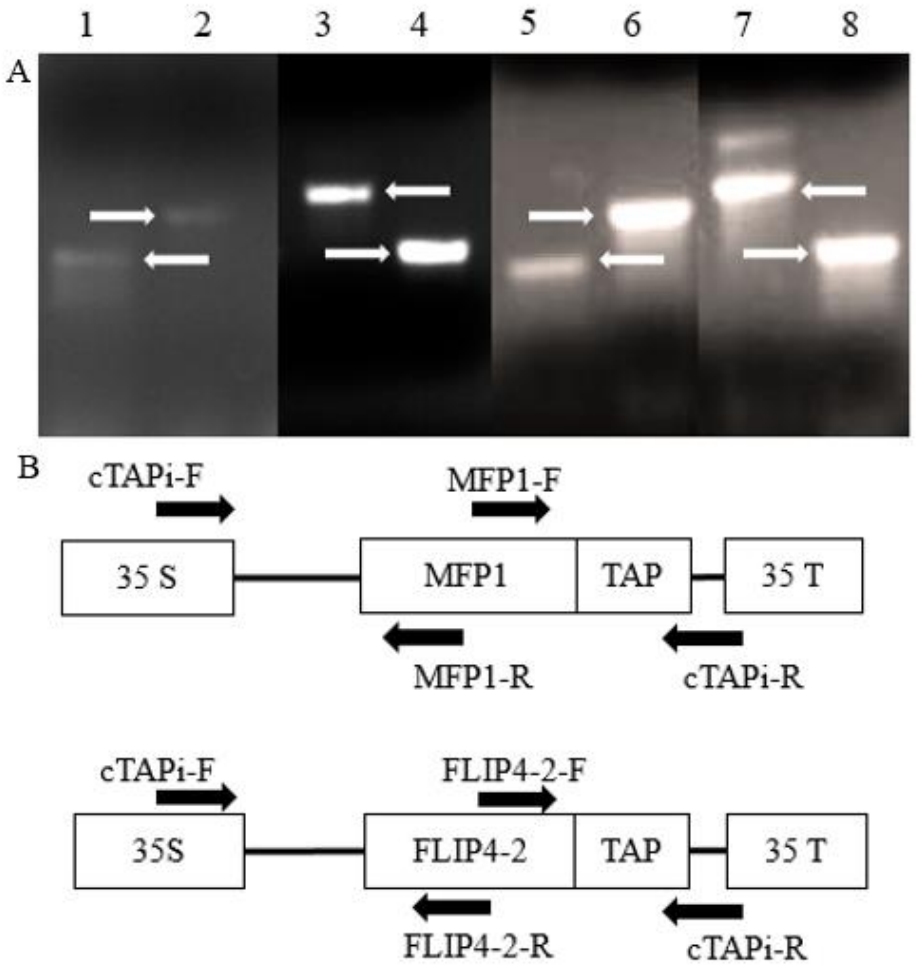

Figure 8. Colony PCR confirmation. A, agarose gel of PCR fragments. Lane 1 confirms cTAPi-Forward/MFP1-Reverse with a band at 707 bp. Lane 2 confirms MFP1-Forward/cTAPi-Reverse with a band at 870 bp. Lane 3 confirms cTAPi-Forward/FLIP4-2-Reverse with a band at 1,168 bp. Lane 4 confirms FLIP4-2-Forward/cTAPi-Reverse with a band at 762 bp. Lane 5-8 represent the positive controls (vector template used for PCR): Lane 5 shows cTAPi-Forward/MFP1-Reverse, lane 6 shows MFP1-Forward/cTAPi-Reverse, lane 7 shows cTAPi-Forward/FLIP4-2-Reverse, and lane 8 shows FLIP4-2-Forward/cTAPi-Reverse PCR products. B, diagram depiction of the MFP1/cTAPi and FLIP4-2/cTAPi expression cassettes. Arrows are showing the location of primers used for confirming the constructs. 35S, CaMV 35S promoter; TAP, tandem affinity purification tag; 35 T, CaMV 35S terminator.

Photosynthesis Analysis

To characterize the possible role of the proteins AtMFP1, AtFLIP4-1, and AtFLIP4-2 in photosynthesis, photosynthetic rates in knock-out mutant plants lacking each protein were measured and compared to the corresponding wild type

Arabidopsis plants. For the AtMFP1 photosynthesis experiment (n=4) the average leaf area for WT WS Arabidopsis plants was 1.0 cm^2/plant ± 0.3 standard error and the AtMFP1 knock-out mutant average leaf area was 2.9 cm^2/plant ± 0.7 (*Figure 9.*). Data from the LiCor photosynthesis experiment were used to generate a photosynthesis light response curve for WT WS and knock-out AtMFP1 mutant plants (*Figure 10.*). The photosynthetic rate for WT WS is higher than for the knock-out AtMFP1 mutant. Photosynthetic photon flux density (PPFD) at 150 $\mu mol/s^{-1}m^{-2}$ was significantly lower in AtMFP1 knock-out mutant plants ($p = 0.024$, with a 95% confidence interval of 0.037 to 0.358) (*Figure 10*). Dark respiration was not significantly different for WT WS than AtMFP1 knock-out mutant plants (2.2 ± 0.5 vs 1.2 ± 0.2, $p = 0.123$). Light compensation point was not significantly different for WT WS than AtMFP1 knock-out mutant plants (32.5 ± 5.8 vs 27.9 ± 3.7, $p = 0.533$). Quantum yield was significantly lower when compared to WT WS than AtMFP1 knock-out mutant plants (0.06 ± 0.007 vs 0.04 ± 0.003, $p = 0.0210$).

For the AtFLIP4 photosynthesis experiment (n=8) the average leaf area for WT Col. Arabidopsis plants were 5.8 cm^2/plant ± 0.8, for AtFLIP4-1 knock-out mutant plants the average leaf area was 4.6 cm^2/plant ± 0.6, and for AtFLIP4-2 knock-out mutant plants the average leaf area was 6.7 cm^2/plant ± 0.7 (*Figure 11.)*. Data from the LiCor photosynthesis experiment were used to generate a photosynthesis light response curve for WT Col., knock-out AtFLIP4-1 mutant plants, and knock-out AtFLIP4-2 mutant plants. The data did not show any significant differences (Table 7).

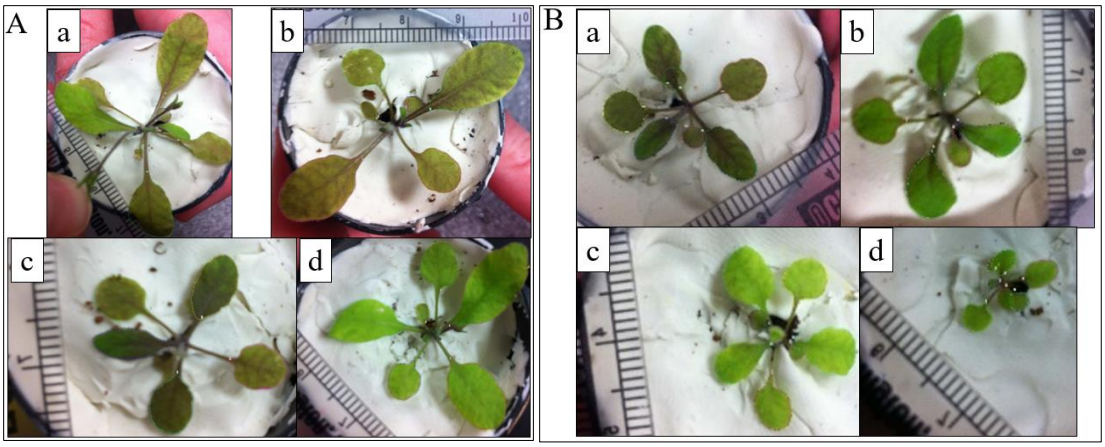

Figure 9. Leaf area photographs MFP1 experiment. A, WT WS plants (a, b, c, and d). B, AtMFP1 knock-out mutant plants (a, b, c, and d)

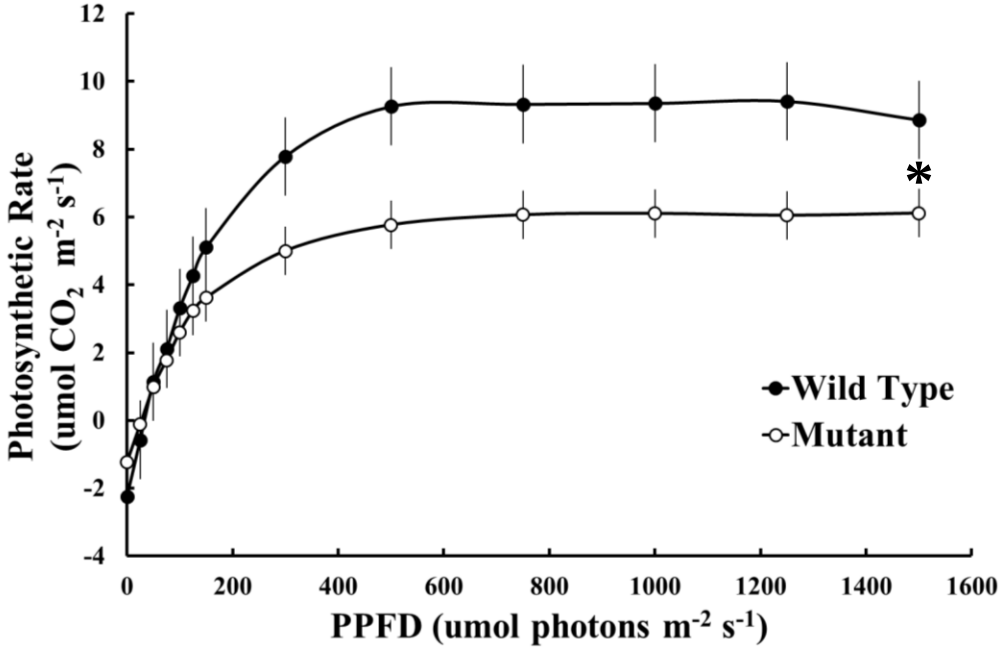

Figure 10. Photosynthesis light response curve. Curve compares WT WS and AtMFP1 knock-out mutant plants. Symbols are means ± standard error, n=4. The asterisk indicates a significant difference at $p < 0.05$.

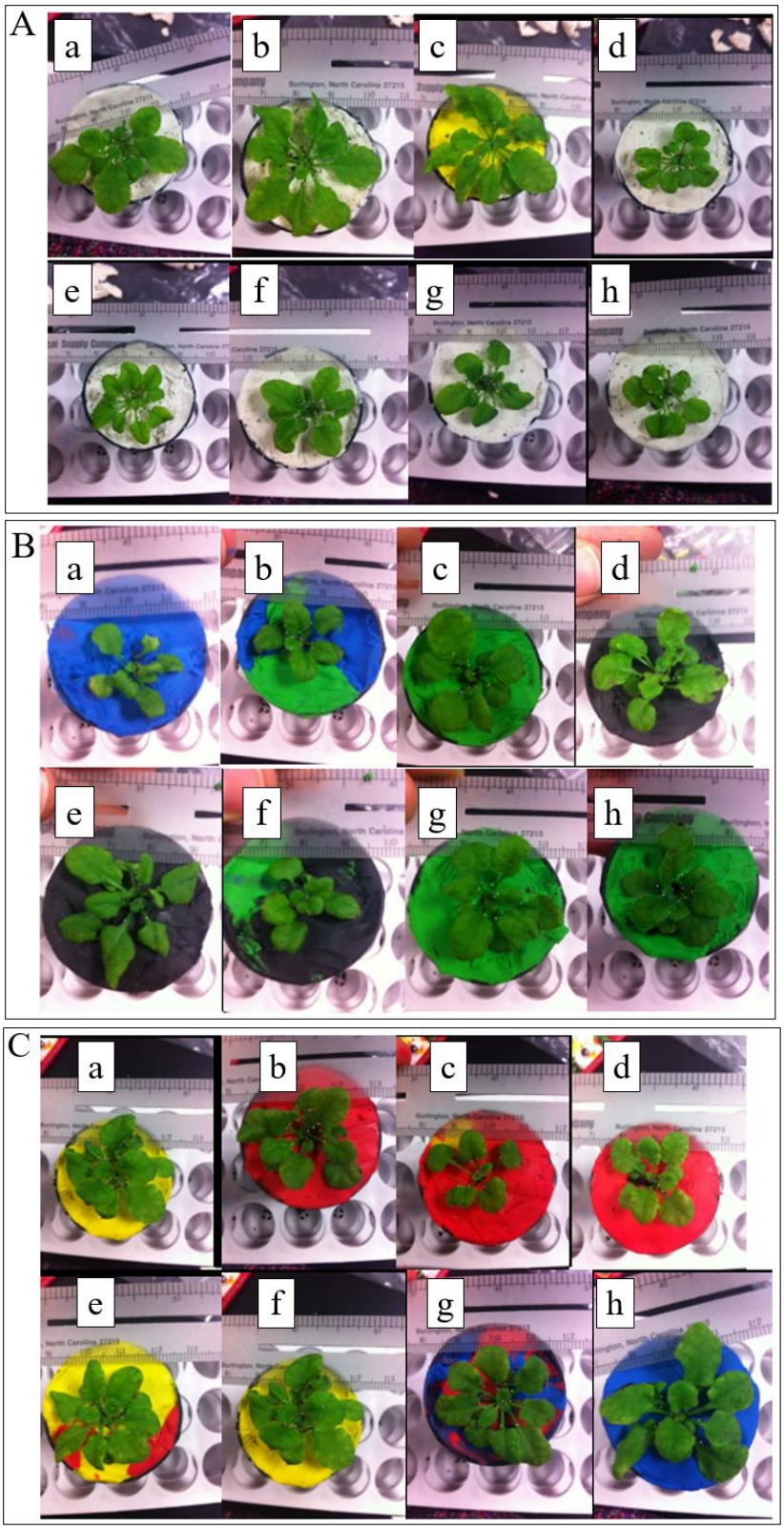

Figure 11. Leaf area photographs FLIP4 experiment. A, wild type (Col.) (a-h) Arabidopsis, B, AtFLIP4-1 knock-out mutant plants (a-h), and C, AtFLIP4-2 knock-out mutant plants (a-h).

Table 7
Max Photosynthesis Measurements ± Standard Error, n=8

genotype	PPFD					
	150		500		1500	
	mean	p-value*	mean	p-value	mean	p-value
F4-1 KO	1.9 ± 0.3	p = 0.81	2.9 ± 0.4	p = 0.90	3.6 ± 0.4	p = 0.90
F4-2 KO	1.5 ± 0.3	p = 0.29	2.4 ± 0.3	p = 0.34	3.0 ± 0.3	p = 0.34
Wild Type	2.0 ± 0.4		3.0 ± 0.5		3.5 ±0.5	

*p-value for comparing either AtFLIP4-1 knock out mutant plants (F4-1 KO) or AtFLIP4-2 knock out mutant plants (F4-2 KO) to wild type Arabidopsis. PPFD = Photosynthetic Photon Flux Density.

Chlorophyll/Carotenoid Content Analysis

Total chlorophyl content was significantly lower in AtMFP1 mutant knock-out plants than wild type WS Arabidopsis plants (17.2 ± 1.2 vs 11.44 ± 1.8, p = 0.039). Chlorophyll *a* content was significantly lower in AtMFP1 mutant knock-out plants than wild type WS Arabidopsis plants (13.4 ± 0.92 vs 8.7 ± 1.4, p= 0.033). There was no statistically significant differences in chlorophyll *b* content in AtMFP1 mutant knock-out plants than wild type WS Arabidopsis plants (3.9 ± 4.0 vs 2.7 ± 0.4, p = 0.100). There was no statistically significant differences in carotenoid content in AtMFP1 knock-out plants than wild type WS Arabidopsis plants (2.5 ± 0.1 vs 1.8 ± 0.3, p = 0.074) (*Figure 12.*).

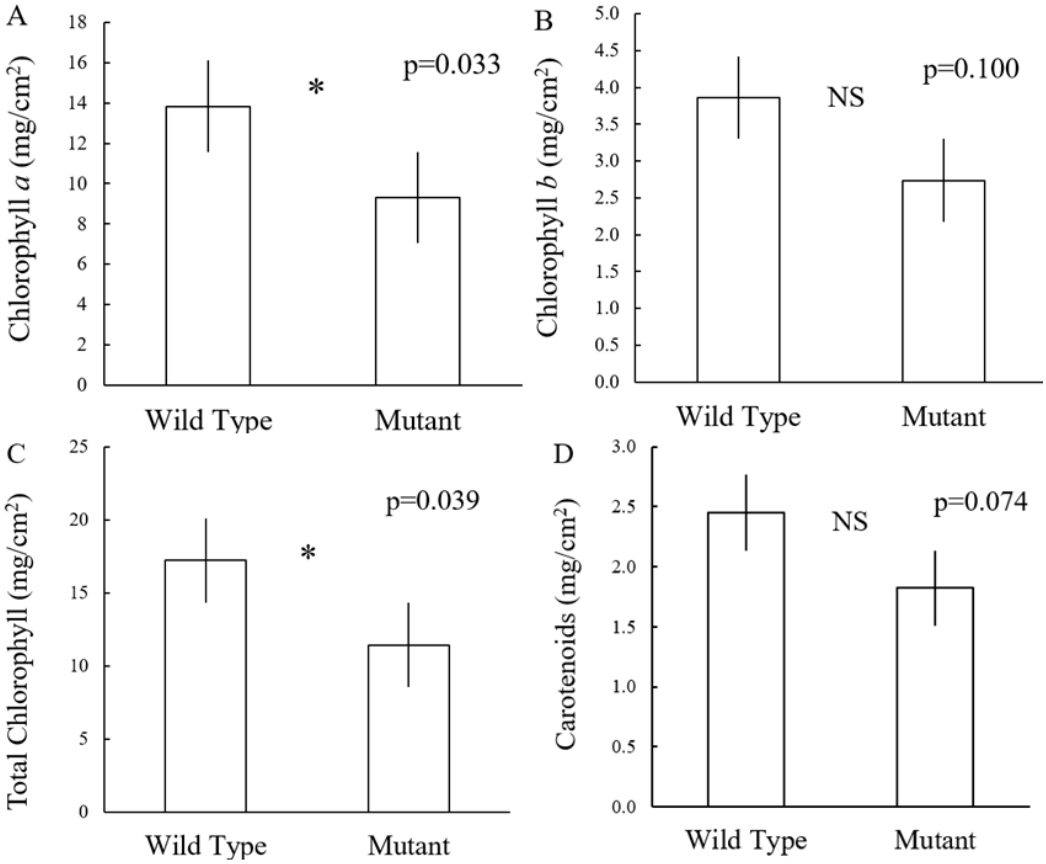

Figure 12. Photosynthetic pigment quantification. Comparing wild type and knock-out mutant plants for AtMFP1. A, Chlorophyll *a*, B, chlorophyll *b*, C, total chlorophyll, and D, carotenoids for AtMFP1. Bars are means ± standard error, n= 4. WT = wild type; Mutant = AtMFP1 knock-out mutant. Asterisks indicate significant difference at $p < 0.05$. NS indicates not significant at $p < 0.05$.

Yeast two-hybrid

AtFLIP4 proteins contain an acidic domain that has been hypothesized to act as a trancriptional activation domain. To confirm that AtFLIP4-2 possesses an activation domain, a yeast two hybrid assay was done. The gene encoding Beta-glucuronidase (GUS) was used as a negative control to replace the *ccdB* gene in the destination vectors. Since GUS is not present in plants, this protein is not expected to interact with any plant proteins. GUS was cloned into the activation domain vector pDEST 22 and GUS was also cloned in the binding domain vector pDEST32. The

vectors pDEST22 and pDEST32 were transformed into competent DB3.1 cells which are resistant to the effects of the *ccdB* gene. The plasmids were isolated and restriction digests with XhoI and NcoI enzymes were used to confirm both plasmid vectors (data not shown). The LR reaction with pENTR™ - gus was utilized to create pDEST22/GUS and pDEST32/GUS. Plasmids were isolated and restriction digest with XhoI and NcoI enzymes were used for both constructs. As expected, based on the vector sequence, the AD-GUS plasmid was digested into 500bp, 1.5 kb, and 7.1 kb fragments by NcoI and XhoI (*Figure 13.*). The BD-GUS plasmid was digested into 374 bp, 1706 bp, and 10.4 kb fragments by NcoI and XhoI as expected based on the vector sequence (*Figure 13.*).

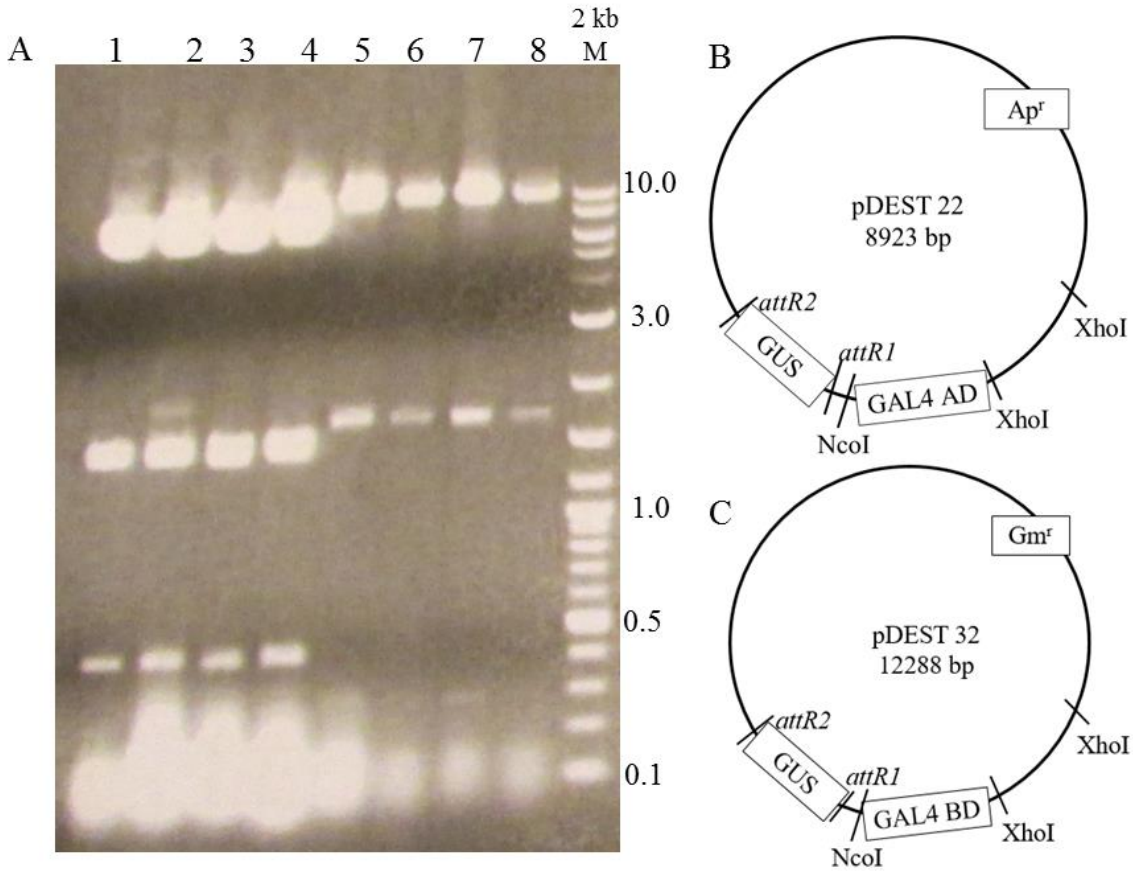

Figure 13. Confirmation of yeast two-hybrid constructs. A, lanes 1-4 represent AD-GUS with fragments at 500 bp, 1.5 kb, and 7.1 kb. Lanes 5-8 represent BD-GUS with fragments at 374 bp, 1706 bp, and 10.425 kb. The figures to the right of the gel are depictions of B, pDEST 22 with Ap^r = ampicillin resistant, restriction digest cuts for NcoI and XhoI, GAL4 AD= transcription factor activation domain, *att* sites flanking the gene of interest GUS and C, pDEST 32 with Gm^r = gentamycin resistant genes, GAL4 BD= transcription factor binding domain.

Yeast two-hybrid constructs were used to test the interaction between AtFLIP4-2 and RanGAP, a known interaction partner of AtFLIP4-2 based on previous yeast two-hybrid experiments, with GUS used as the negative control. Yeast strains YRG-2 and PJ69-A4 were transformed with BD-RanGAP + AD-FLIP4-2 (interaction positive control), BD-FLIP4-2 + AD-GUS (negative control), and BD-GUS + AD-FLIP4-2 (activation domain test). Yeast colonies were present on each plate tested on SD-Leu/-Trp plates (data not shown). Colonies from each

transformation were streaked onto –Leu/-Trp/-His dropout plates to detect reporter gene activation.

The interactions tested for AD-FLIP4-2 plus BD-RanGAP showed growth of yeast on SD-Leu/-Trp/-His plates (*Figure 14.*) confirming interaction between AtFLIP4-2 and RanGAP. The negative control for interactions testing AD-FLIP4-2 plus BD-GUS did not show any growth of yeast on SD-Leu/-Trp/-His plates (*Figure 14.*) confirming that AtFLIP4-2 does not interact with GUS. The activation test for BD-FLIP4-2 plus AD-GUS showed growth of yeast on SD-Leu/-Trp/-His plates (*Figure 14.*); this result suggests the presence of an activation domain on AtFLIP4-2 (Table 8).

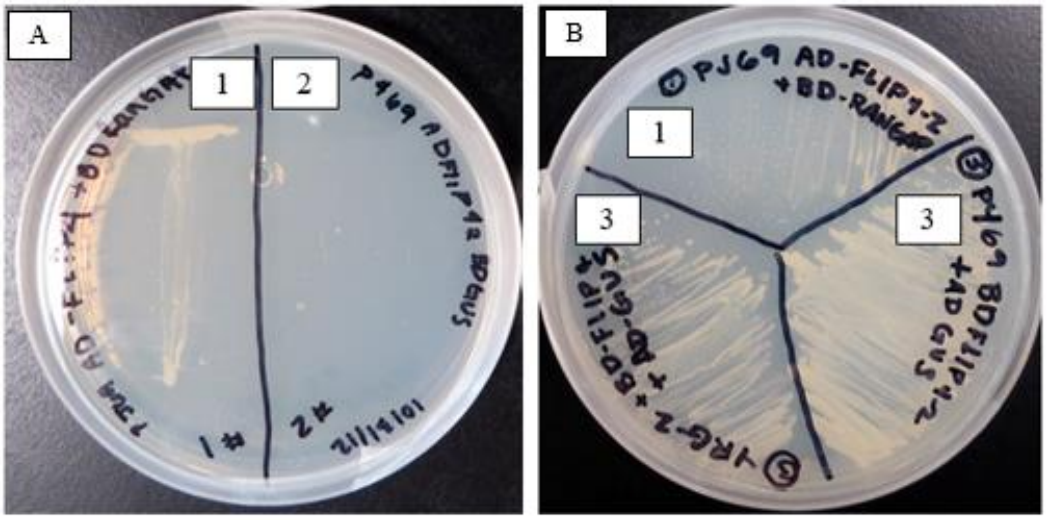

Figure 14. Yeast two-hybrid analysis. A. 1) Growth is present for AD-FLIP4-2 + RanGAP (yeast PJ69-A4) appears. A. 2) No growth is present for AD-FLIP4-2 + GUS. B. 1) Growth is present for AD-FLIP4-2 + BD-RanGAP. B. 3) Growth is present for BD-FLIP4-2 + AD-GUS (yeast YRG-2 left, yeast PY69-A4 right).

Table 8
Yeast Two-Hybrid Constructs, Growth, and Outcome

Constructs	Growth	Outcome
1. AD-FLIP4-2 + BD-RanGAP	++	interaction
2. AD-FLIP4-2 + BD-GUS	- -	negative control, no interaction
3. BD-FLIP4-2 + AD-GUS	++	activation by BD-FLIP4-2

Bioinformatics Analysis of AtFLIP4-1 and AtFLIP4-2 interaction networks

A proteome-wide binary protein-protein interaction study was published in 2011 for the interactome network of Arabidopsis which found about 6,200 highly reliable interactions between about 2,700 proteins using yeast two-hybrid analysis (Arabidopsis Interactome Mapping Consortium 2011). AtFLIP4-2 (At5g66480) and AtFLIP4-1 (At3g50910), comprising the FLIP4 gene family in Arabidopsis, where a part of the mapping consortium data. Thirty two proteins were identified to interact with AtFLIP4-1 (Table 9) and twelve proteins were identified to interact with AtFLIP4-2 (Table 10).

Table 9
Potential AtFLIP4-1 Protein-Protein Interaction Partners

Protein	Name	Predicted Location
AT3G01550	PPT2 (PHOSPHOENOLPYRUVATE (PEP)/PHOSPHATE TRANSLOCATOR 2); antiporter/ triose-phosphate transmembrane transporter	Chloroplast
AT5G20130	unknown	Chloroplast
AT4G02725	unknown	Chloroplast
AT2G43370	U1 small nuclear ribonucleoprotein 70 kDa, putative	unknown
AT5G65683	zinc finger (C3HC4-type RING finger) family protein	unknown
AT1G06390	ATGSK1 and GSK1, GSK1 (GSK3/SHAGGY-LIKE PROTEIN KINASE 1); glycogen synthase kinase 3/ kinase	unknown
AT3G60600	(AT)VAP and VAP and VAP27 and VAP27-1, VAP (VESICLE ASSOCIATED PROTEIN); protein binding	unknown
AT5G17630	glucose-6-phosphate/phosphate translocator, putative	Chloroplast
AT3G20510	unknown	unknown
AT3G13175	unknown	unknown
AT5G51010	rubredoxin family protein	Chloroplast
AT2G42260	PYM and UVI4, UVI4 (UV-B-INSENSITIVE 4)	unknown
AT3G60360	EDA14 and UTP11, EDA14 (EMBRYO SAC DEVELOPMENT ARREST 14)	unknown
AT2G36990	SIG6 and SIGF, SIGF (RNA POLYMERASE SIGMA-SUBUNIT F); DNA binding / DNA-directed RNA polymerase/ sigma factor/ transcription factor	Chloroplast
AT3G11590	unknown	Chloroplast
AT5G45420	myb family transcription factor	ER
AT1G04340	lesion inducing protein-related	unknown
AT3G51510	unknown	Chloroplast; exp, Chloroplast thylakoid
AT1G54770	unknown	unknown
AT3G63130	RANGAP1, RANGAP1 (RAN GTPASE ACTIVATING PROTEIN 1); RAN GTPase activator/ protein binding	unknown
AT1G53800	endonuclease	Chloroplast
AT4G20300	unknown	unknown
AT1G79040	PSBR (photosystem II subunit R)	Chloroplast; exp, Chloroplast thylakoid
AT3G60200	unknown	unknown
AT5G05760	ATSED5 and ATSYP31 and SED5 and SYP31, SYP31 (SYNTAXIN OF PLANTS 31); SNAP receptor	unknown
AT2G31040	unknown	Chloroplast
AT2G20920	unknown	Chloroplast
AT2G20060	ribosomal protein L4 family protein	Mitochondrion
AT2G32840	proline-rich family protein	Chloroplast
AT5G17450	heavy-metal-associated domain-containing protein / copper chaperone (CCH)-related	unknown

Table 10
Potential AtFLIP4-2 Protein-Protein Interaction Partners

Protein	Name	Predicted Location
AT3G50920	phosphatidic acid phosphatase-related / PAP2-related	Chloroplast
AT3G60590	unknown protein	Chloroplast, chloroplast inner membrane, chloroplast envelope
AT5G67210	unknown protein	unknown
AT1G14360	ATUTR3 and UTR3, UTR3 (UDP-GALACTOSE TRANSPORTER 3); pyrimidine nucleotide sugar transmembrane transporter	endomembrane system
AT3G58170	ATBET11 and ATBS14A and BET11, BS14A (BET1P/SFT1P-LIKE PROTEIN 14A); SNAP receptor/ protein transporter	Golgi apparatus, nucleus, plasma membrane
AT3G01660	methyltransferase	unknown
AT2G14860	peroxisomal membrane protein 22 kDa, putative	Peroxisomal membrane
AT5G05760	ATSED5 and ATSYP31 and SED5 and SYP31, SYP31 (SYNTAXIN OF PLANTS 31); SNAP receptor	Golgi apparatus, cell plate, intracellular membrane-bounded organelle

note: RanGAP (At3g63130) was confirmed to interact with AtFLIP4-2, demonstrated by the yeast two-hybrid analysis presented in this thesis.

To further investigate the AtFLIP4-1 and AtFLIP4-2 potential protein interaction partners from this analysis, I used the BAR Arabidopsis Interaction Viewer (Waese et al. 2017) to construct an interaction map with colored prediction boxes on the location of the partners in the Arabidopsis plant cell (*Figure 15.*). The BAR Arabidopsis Interaction Viewer depicted the interaction of AtRanGAP At3g6130 only with AtFLIP4-1; however, based on my yeast two-hybrid data AtRanGAP also interacts with AtFLIP4-2 in yeast two-hybrid assays. All predicted AtFLIP4-1 interactions were part of the large-scale yeast two-hybrid analysis except for ATR13_group which was part of a mapping of a plant-pathogen protein-protein interactome network (Mukhtar et al. 2011). All predicted AtFLIP4-2 interactions were part of the large-scale yeast two-hybrid analysis except for At3g11820, HARXLL495, HARXLL492, and HARLL149 which were part of a mapping of a

plant-pathogen protein-protein interactome network (Mukhtar et al. 2011). The protein encoded by the plant gene At5g05760 was found to interact with both AtFLIP4-1 and AtFLIP4-2 and has a predicted localization in the Golgi apparatus. The protein encoded by the plant gene At5g67210, which interacts with AtFLIP4-2, was predicted to be localized in the chloroplast using ChloroP but did not depict a localization in the plastid with the BAR Arabidopsis Interaction Viewer (*Figure 16.* and Table 11).

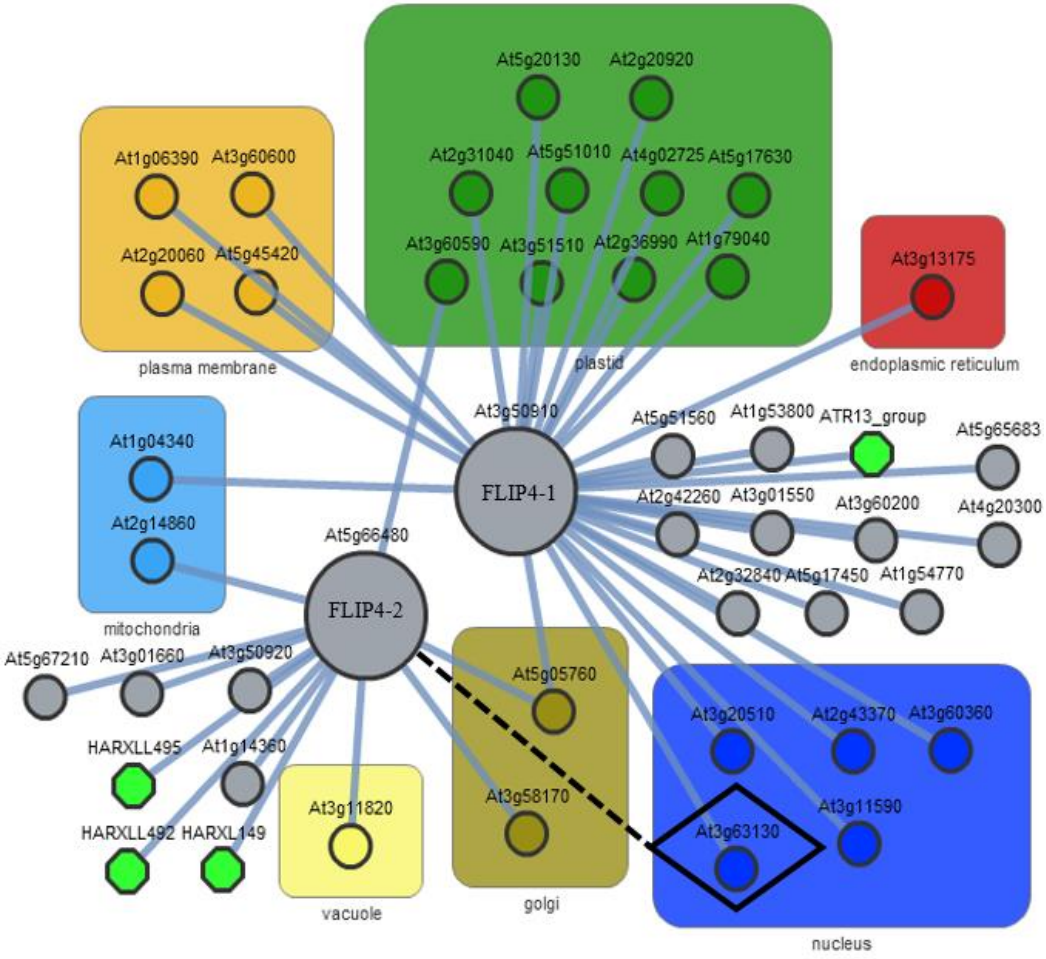

Figure 15. Potential protein interaction partners for AtFLIP4. Note the dashed line connecting AtRanGAP At3g63130 to AtFLIP4-2, which is based on the yeast two-hybrid experiment performed in this thesis.

For the AtFLIP4-2 potential binding proteins I utilized the Multicoil program to predict if the potential binding partner has a coiled coil motif, and the ChloroP and TargetP programs to predict if the potential binding partner is in the chloroplast (Table 11). Two hypothetical proteins encoded by the genes At3g60590 and At5g67210 are predicted to co-localize with AtFLIP4-2 in the chloroplast.

Table 11
Bioinformatics Data on Potential AtFLIP4-2 Interaction Partners

Accession Number	Description	Multicoil Coiled-Coil	ChloroP cTP	TargetP
At3g50920	Phosphatidic acid phosphatase (PAP2) family protein	no	no	ND
At3g01660	S-adenosylmethionine-dependent methyltransferase domain-containing protein	no	no	mitochondria
At2g14860	Protein Mpv17	no	no	mitochondria
At3g60590	hypothetical protein length: 166, score: 0.537 cTP: Y CS-score: -1.962, cTP-length: 74	no	yes*	ND
At3g58170	Bet1-like SNARE 1-1 UDP-galactose transporter 3	no	no	ND
At1g14360	length: 317, score: 0.523, cTP: Y CS-score: -2.251, cTP length: 48	no	yes*	ND
At5g05760	syntaxin-31	no	no	ND

**note:* At3g60590 and At5g67210 are predicted to be located in the chloroplast.

To further visualize localization of AtFLIP4-1 and AtFLIP4-2 I used the BAR Arabidopsis viewer which creates localization intensities in Arabidopsis plant parts and tissues based on localization predictions and available microarray expression data (*Figure 16.*). AtFLIP4-1 is predicted to localize in the nucleus (*Figure 16.* A) and is highly expressed in the guard cells (*Figure 16.* C), pollen and specifically in the

sperm cell. AtFLIP4-2 is predicted to localize in the chloroplast (*Figure 16.* B), but no expression data were available as the AtFLIP4-2 gene is not represented by any probes on the commonly used ATH1 microarray chips (Affymetrix) for Arabidopsis.

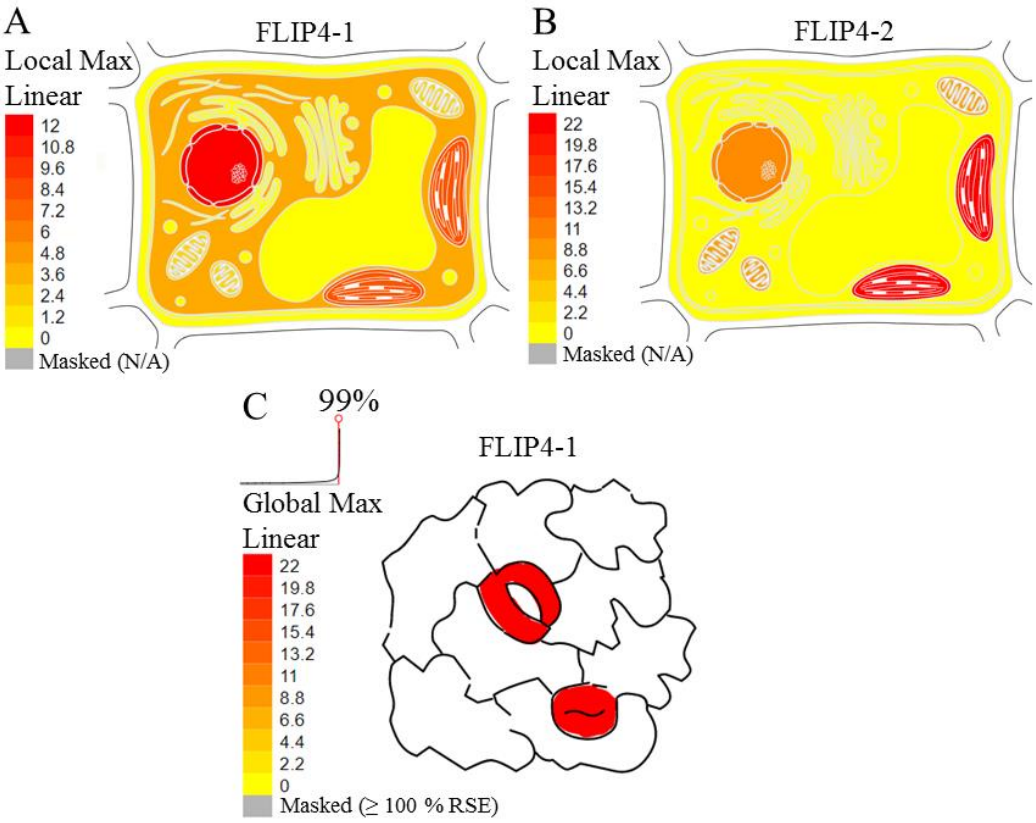

Figure 16. Localization visualization of AtFLIP4-1 and AtFLIP4-2. A, the top left depiction is the predicted localization of AtFLIP4-1 in the nucleus. B, the top right depiction is the predicted localization of AtFLIP4-2 in the chloroplast. C, the bottom depiction is the expression of AtFLIP4-1 in the guard cells.

Further Study of AtFLIP4 Gene Family Interaction Partners

Available cDNA clones and knock-out Arabidopsis mutant seeds of the potential binding partners of AtFLIP4-1 and AtFLIP4-2 are presented in Table 12. The objective of this study was to clone the cDNAs for putative interaction partners for further study.

Table 12
Available cDNA Clones for AtFLIP4 Interaction Partners

Protein of Interest	Accession Number	cDNA[A]	T-DNA mutant[B]
AtFLIP4-2	At3g50920*	C62603	None Available
	At3g60590	U17386	006242C
	At5g67210*	U22824	None Available
AtFLIP4-1	At1g79040*	U11815	None Available
	At2g20920*	U21287	None Available
	At2g31040	U13452	057229
	At5g20130	U68182	None Available
	At4g02725	U68182	None Available
	At5g17630	U12352	None Available
	At2g36990	U11195	None Available
	At5g51010	U10308	None Available

*cDNA clones successfully transformed into D-TOPO vector and confirmed through sequencing.
[A]cDNA stocks in pUni51 cloning vector obtained from ABRC
[B]Seed stocks for SALK T-DNA mutant lines obtained from ABRC

Clones containing the cDNAs were confirmed using restriction digest and gel electrophoresis (Table 13, *Figure 17.*). All cDNAs were confirmed, except U68501, by observing their predicted band fragments.

Table 13
Restriction Enzymes and Buffers Used to Confirm cDNA Clones for AtFLIP4 Interaction Partners

Accession Number	**cDNA**	**Restriction Enzyme(s)**	**Buffer**	**Expected Fragments (bp)**
At3g50920	C62603	EcoRI	EcoRI	2975, 448, 309
At3g60590	U17386	XbaI, EcoRI	2	2346, 706
At5g67210	U22824	AatII, EcoRI	4	2799, 706
At1g79040	U11815	EcoRI	EcoRI	2831, 503
At2g20920	U21287	EcoRI	EcoRI	2351, 1074, 551
At2g31040	U13452	SpeI	2	2704
At5g20130	U68501	HindIII	2	2135, 1023
At4g02725	U68182	NcoI, EcoRI	4	2610, 434
At5g17630	U12352	KpnI	1	2796, 784, 228
At2g36990	U11195	NcoI, EcoRI	4	3523, 706
At5g51010	U10308	SalI, EcoRI	3	2344, 706

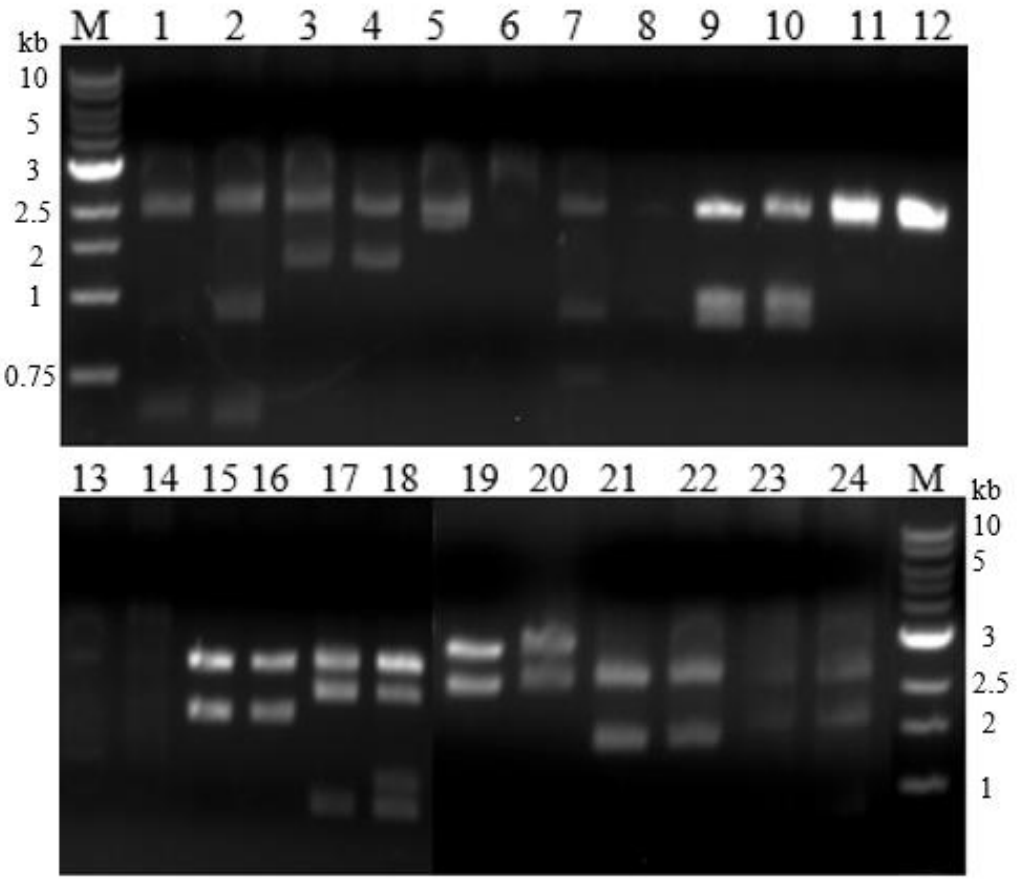

Figure 17. Confirmation of cDNA clones for AtFLIP4 binding partners. M = 1kb marker. Lane 2 confirms C62603, lanes 3 and 4 confirm U17386, lane 5 confirms U22824, lane 7 confirms U11815, lane 9 and 10 confirm U21287, lane 11 and 12 confirm U13452, lane 15 and 16 confirms U68182, lane 17 confirms U12352, lane 19 confirms U11195, lane 21 and 22 confirms U10308, lane 23 and 24 confirm AtFLIP4-1. Lanes 1, 6, 8, 18, and 20 did not confirm. Lane 13 and 14 did not confirm U68501.

Primers were designed to amplify the open reading frames without stop codons and PCR was performed with all the confirmed cDNAs followed by gel purification on all PCR products (*Figure 18.* and Table 3 and 4).

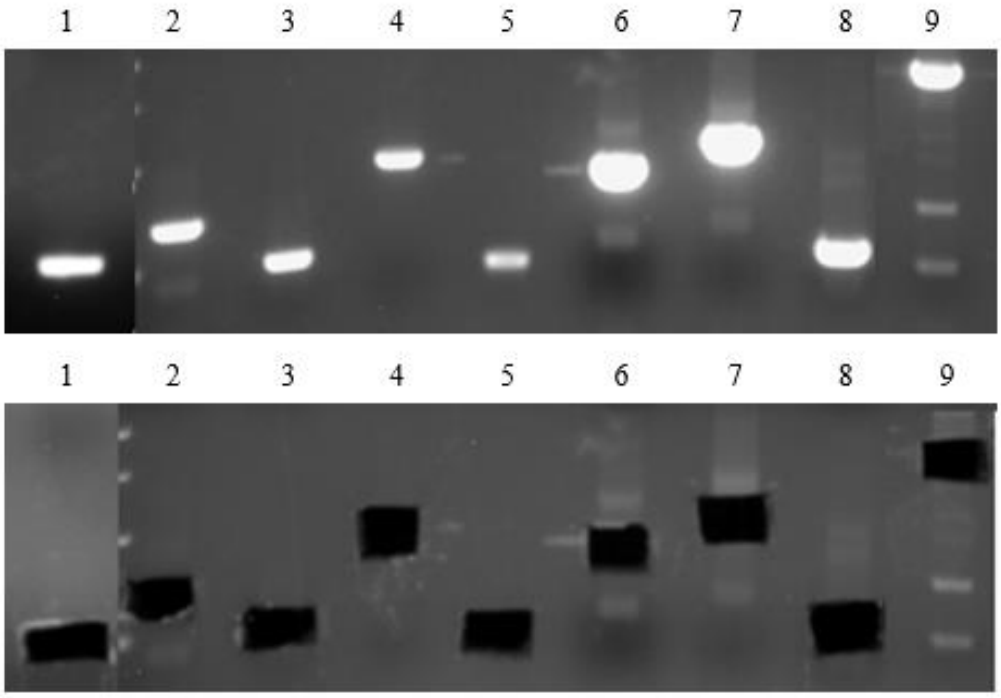

Figure 18. Gel purification of cDNA clones for AtFLIP4 binding partners. Lane 1 = U10308, lane 2 = C62603, lane 3 = U17386, lane 4 = U22824, lane 5 = U11815, lane 6 = U21287, lane 7 = U13452, lane 8 = U68182, and lane 9 = U11195. The top photo is before the bands were cut out and the bottom photo confirmed that the entire band was removed.

The TOPO-cloning reaction was completed on all purified DNA. cDNA/D-TOPO/*E.coli* U11195 did not grow in culture and was not used for continued work. Mini preps, restriction digest, and gel electrophoresis confirmed the cDNA/D-TOPO vectors (*Figure 19.*). The confirmed cDNA/D-TOPO plasmid vectors were sent out for sequencing (Table 12). The cloned cDNAs for putative interaction proteins for AtFLIP4-1 and AtFLIP4-2 are ready for further study.

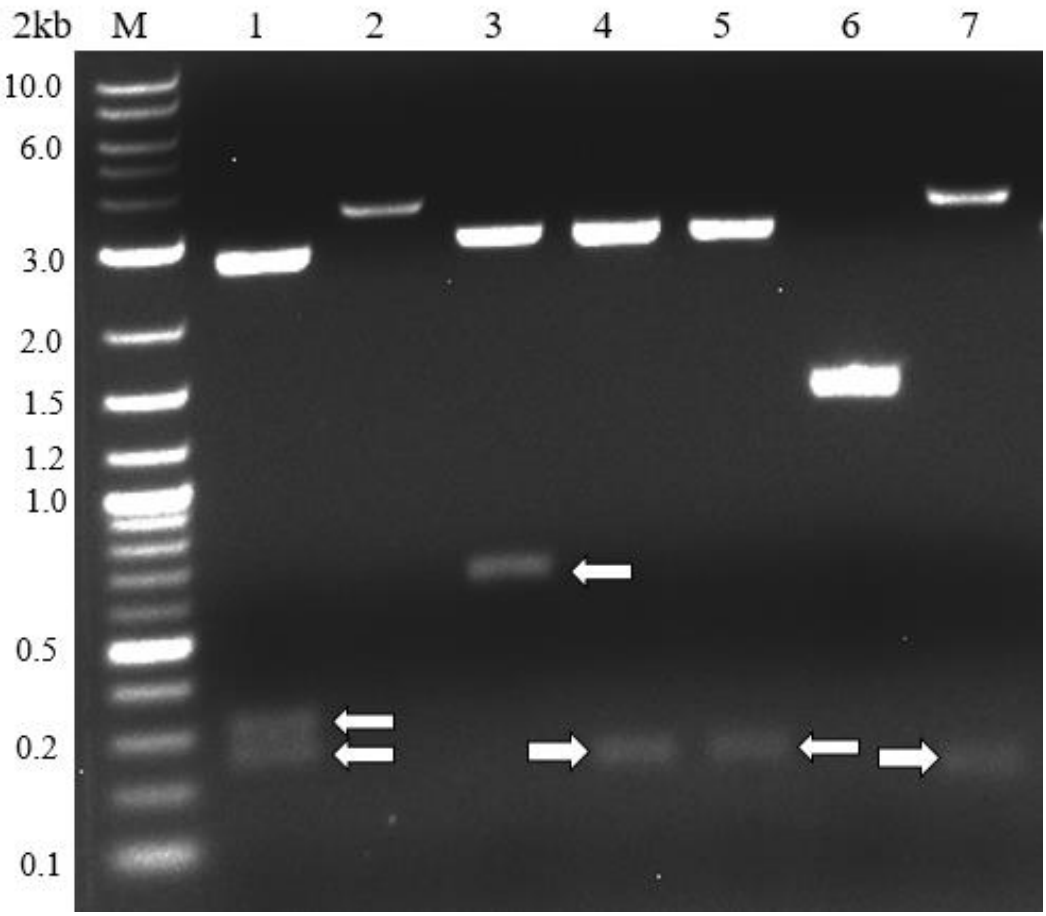

Figure 19. Confirmation of cDNA/D-TOPO plasmid vectors. Lane 1 = C62603, lane 2 did not confirm, lane 3 = U22824, lane 4 and 5 = U11815, lane 6 did not confirm, lane 7 = U21287.

Discussion

Arabidopsis AtFLIP4-2 Interacts with RanGAP and Activates Transcription in Yeast

FLIP4 was originally identified in tomato in a yeast two-hybrid screen with MFP1 associated factor 1 (MAF1) (Patel et al. 2005). MAF1 is localized to the nuclear envelope and shares a targeting domain with RanGAP. Plant RanGAP assists in nuclear import of proteins targeted to the nuclear pore (Meier et al. 2010). Arabidopsis contains two homologs of tomato FLIP4 due to a recent genome duplication in Brassicaceae (Reel 2013; Cole 2014; Judge 2015). AtFLIP4-2 has been confirmed to interact with tomato MAF1, but not with its Arabidopsis homologs, and with RanGAP in yeast two-hybrid assays. Yeast two-hybrid analysis is an appropriate tool to identify protein interaction partners (Criekinge and Beyaert 1999). AtFLIP4-2 was also predicted to have an activation domain based on an acidic domain in the protein. Utilizing the yeast two-hybrid technology, the presence of an activation domain in AtFLIP4-2 and interactions between AtRanGAP and AtFLIP4-2 were tested with the constructs in Table 8. AtFLIP4-2 and AtRanGAP confirmed an interaction through yeast two-hybrid analysis (*Figure 14.*) while the lack of colonies on selection plates for AtFLIP4-2 and GUS confirmed that these proteins do not interact. GUS is not present in higher plants and therefore was chosen as a suitable negative control in AD or BD fusion constructs and to replace the *ccdB* gene in the destination vectors. Growth was present from the assay BD-FLIP4-2 + AD-GUS, suggesting that AtFLIP4-2 possesses an activation domain because it is able to activate reporter gene expression when fused to the binding domain in absence of

interaction with the AD fusion protein (*Figure 14.*). Taken together, the yeast two-hybrid analysis provided further evidence of the interaction of AtFLIP4-2 and AtRanGAP and that AtFLIP4-2 possesses an activation domain. Plastid envelope membrane proteins may play a role in expression of the plastid genome (Sato et al. 1999). For example, the protein Plastid Envelope DNA binding (PEND), like FLIP4-2, is shown to be a plasmid envelope protein and binds DNA (Sato et al. 1998).

AtFLIP4-1 and AtFLIP4-2 are Part of a Protein-Protein Interaction Network in Arabidopsis

AtFLIP4-1 and AtFLIP4-2 were part of a large yeast two-hybrid screen (Arabidopsis Interactome Mapping Consortium 2011). By analyzing the information from this screen, potential protein binding partners for AtFLIP4-1 and AtFLIP4-2 were found (Table 9 and Table 10). Bioinformatics tools were then used to test potential interaction partners for AtFLIP4-2 for coiled-coil motifs, localization in the chloroplast, and predictions of subcellular location of proteins (Table 11). Hypothetical proteins encoded by At3g60590 and At1g14360 and associated with AtFLIP4-2 were predicted to be localized in the chloroplast; therefore, they are the best candidates to be true interaction partners in the chloroplast (Table 11). The At3g60590 gene product HP36b is annotated as an inner chloroplast membrane protein and was found in a proteomics study of the Arabidopsis chloroplast envelope (Ferro et al. 2003). This confirms its predicted localization and makes it the best candidate of the proteins identified to co-localize with AtFLIP4-2 at the inner membrane of the chloroplast envelope. However, its function is unknown and thus provides no further clue to AtFLIP4-2 function. The At1g14360 gene product is

annotated as an integral membrane protein of the endoplasmic reticulum or Golgi apparatus and less likely to be truly localized in the chloroplast. It is noteworthy that both of these putative interaction partners are membrane-associated proteins. At3g01660, coding for S-adenosylmethionine-dependent methyltransferase domain-containing protein, and At2g14860, coding for the peroxisomal membrane protein Mpv17, associated with AtFLIP4-2 are predicted to be localized in the mitochondria (Table 11). Mitochondrial and chloroplast proteins often show dual localization, so they would be good candidates as well. However, the annotation of Mpv17 as peroxisomal membrane protein illustrates the error-prone nature of computational localization predictions.

AtFLIP4-1 and AtFLIP4-2 were also analyzed through the BAR Arabidopsis protein interaction viewer to construct an interaction map with colored prediction boxes on the possible localization of protein interaction partners (*Figure 15.*). The protein AtRanGAP was found to interact with AtFLIP4-1; however, the large yeast two-hybrid screen and the interaction viewer failed to identify the protein-protein interaction of AtRanGAP with AtFLIP4-2, this thesis work, however, confirmed interaction through yeast two-hybrid analysis (*Figure 15.*). Taken together, this suggests AtRanGAP as a shared interaction partner for both AtFLIP4-1 and AtFLIP4-2. However, since AtRanGAP is located at the nuclear pore the significance of this interaction for chloroplast function is unclear. Another notable find is the shared interaction of the SNARE protein encoded by At5g05760 with AtFLIP4-1 and AtFLIP4-2. This protein, also known as Syntaxin of Plants (SYP) 31, is located at the Golgi apparatus and functions in vesicle trafficking in the secretory pathway (Bubeck

et al. 2008). It has a structure typical of golgin proteins with a coiled-coil domain followed by a C-terminal transmembrane domain, similar to the structure of the FLIP4 proteins. It was hypothesized based on studies of the GeneMANIA network that AtFLIP4-2 plays a role in intra-Golgi vesicle-mediated transport (Judge 2015). Based on similarity with SNARE proteins and interaction with a Golgi protein involved in vesicle trafficking, we hypothesize that AtFLIP4-1 and AtFLIP4-2 may be involved in vesicle-mediated transport aiding the evolution of land plants. AtFLIP4-1 is predicted to be localized in the guard cells of plants, which could link functionality of AtFLIP4-1 to responses to drought conditions as plants evolved from water to land (*Figure 19.*). Genes co-expressed with AtFLIP4-1 have also been identified to include transcription factors that played a role in drought, heat, and oxidative stresses (The Arabidopsis Genome Initiative 2000; Judge 2015). Also, putative drought and Abscisic acid response element motifs have been detected in the promoter regions of AtFLIP4-1 and AtFLIP4-2 (Cole 2014). AtFLIP4-2 as an inner chloroplast membrane protein and may be involved in plastidic vesicle transport from the inner membrane to the thylakoid membrane similar to the protein VIPP1 (Kroll et al. 2001). This research supports the hypothesis that during the evolution of land plants AtFLIP4-1 and AtFLIP4-2 played a role in water retention in plants transitioning from water to land and the evolution of the eukaryotic-type features of land plant chloroplasts by attaching chloroplast targeting domains to proteins originally located in other organelles such as the Golgi apparatus.

Further Studies of AtFLIP4-1 and AtFLIP4-2 Interaction Partners

Due to the unreliable nature of targeting predictions and yeast two-hybrid interactions, further studies are needed to evaluate the localization and interaction properties of the putative AtFLIP4 interaction partners. Available cDNA clones of the potential binding partners of AtFLIP4-1 and AtFLIP4-2, identified through the large yeast two-hybrid study, were transformed into the ENTR clone D-TOPO (Table 12). Future experiments can be done to further investigate if these proteins interact *in planta* through bimolecular fluorescence complementation (BiFC) split-green fluorescent protein (GFP) analysis. This method involves creating an N-terminal domain fragment of GFP fused to AtFLIP4 and a C-terminal domain fragment of GFP fused to each potential protein interaction partner, which are then transformed into plant cells to test for interaction and localization *in planta* (Bracha-Drori et al. 2004; Magliery et al. 2004). When the two fragments of GFP are each individually fused to the interaction proteins the reassembly of the GFP can take place (Jackrel et al. 2010). Not only can BiFC split-GFP determine location and interaction of protein-protein partners, it is also possible to measure the magnitude of the fluorescent intensity that is generated by the mature formation of GFP after fusion to determine the extent of the protein-protein interaction *in planta.* This work has provided the starting material for BiFC split-GFP which can be used to further analyze the potential protein-protein binding partners for AtFLIP4-1 and AtFLIP4-2 and confirming their interactions *in planta*.

Identification of Chloroplast-localized Interaction Partners of AtMFP1 and AtFLIP4-2

Previous attempts to find MFP1 interaction partners through yeast two-hybrid analyses did not identify chloroplast proteins. This may be because yeast is a heterologous system and all activation domain/binding domain fusion proteins contain a nuclear localization signal to import into the nucleus. Thus, proteins usually found in different organelles in the plant cell are brought together, resulting in possible false positive interactions that are relevant for plant cell function. To identify chloroplast-localized binding proteins of AtMFP1 and AtFLIP4-2, I cloned constructs for tandem affinity purification (TAP) which can be used in combination with mass spectrometry (MS) to identify chloroplast protein-protein interaction complexes. The TAP tagging method is an efficient system for identifying *in vivo* protein interaction partners (Xu et al. 2010). I cloned the cDNA for AtMFP1 into Gateway pENTR vector (*Figure 5.*) and confirmed it through sequencing (*Figure 6.*). Then by using the MFP1/pENTR vector and the AtFLIP4-2/pENTR vector the LR reaction was used to successfully clone the cDNAs for the proteins of interest into the cTAPi vector (*Figure 7.*). *A. tumefaciens* GV3101 was transformed with MFP1/cTAPi or FLIP4-2/cTAPi plasmid vectors and confirmed by colony PCR (*Figure 8.*). These transformed bacteria have formed the basis for plant transformation to generate transgenic lines expressing TAP-tagged AtMFP1, which will be used in a follow-up project to isolate AtMFP1-containing protein complexes from chloroplasts.

AtMFP1 Mutants Show Reduced Photosynthetic Efficiency Under Stress Conditions

Arabidopsis thylakoid membrane proteins that do not have apparent cyanobacterial homologs, such as AtMFP1, may be involved in the evolutionary adaptations of photosynthetic processes in land plants. MFP1 is an integral membrane protein of the chloroplast thylakoid membrane and highly expressed in green, photosynthetic tissues in tomato (Jeong et al. 2003). Blue Native polyacrylamide gel electrophoresis (BN-PAGE) showed AtMFP1 associated with the photosystem-II-light harvesting complex-II (PSII-LHCII) super complexes (Havighorst 2012). AtFLIP4-2 is thought to be located in the chloroplast envelope and is predicted to be an integral membrane protein that could be involved in vesicle transport to form thylakoids (*Figure 16.)* (Richardson 2012). A possible function of AtMFP1and AtFLIP4-2 is their direct or indirect involvement in the photosynthetic processes. Due to MFP1 associating with the thylakoid membrane and recent work suggesting its involvement with photosynthetic complexes, photosynthesis measurements would hypothetically be altered in plants lacking AtMFP1. If FLIP4 proteins are involved in vesicle-mediated formation of the thylakoid membrane, they also could have an effect on photosynthesis.

AtMFP1 knock-out mutant plants when compared to wild type Arabidopsis plants showed significant differences in photosynthetic rates. It should be noted that the plants used in the photosynthesis measurements, chlorophyll and carotenoid AtMFP1 experiment appeared small and slightly sickly (*Figure 10.*). Photosynthesis measurement at 150 μmol m^{-2} s^{-1}PPFD, apparent, and Chlorophyll (*a* and total) were

significantly lower in AtMFP1 knock-out mutant plants when compared to wild type (*Figure 14.).* However, another researcher repeated this same experiment with healthier looking larger plants with a larger sample size of six wild type and six AtMFP1 knock-out mutant plants instead of four wild type and four AtMFP1 knock-out mutant plants and did not show any significant differences between mutant and wild type. It has been hypothesized that MFP1 functions under drought stress (Jeong et al. 2003). Therefore, since the plants in this experiment were small and looked unhealthy this could indicate a stress condition which the knock-out AtMFP1 mutant plants could not overcome which led to these statistically significant results. Further research will need to be explored to understand this potential phenotype under stress conditions and to determine what type of stress is responsible.

There were no significant differences found in knock-out AtFLIP4-1 and AtFLIP4-2 plants when compared to wild type Arabidopsis plants at 150 µmol m^{-2} s^{-1} PPFD, 500 µmol m^{-2} s^{-1} PPFD, and 1500 µmol m^{-2} s^{-1} PPFD (Table 7.). This could be due to redundancy following a recent gene duplication event in Arabidopsis since the divergence of the Brassicaceae family (Barker et al. 2009; Flagel and Wendel 2009; Monson 2003). Since AtFLIP4-1 and AtFLIP4-2 are products of a recent gene duplication event, it is not surprising that they exhibit redundant functions. Therefore, AtFLIP4-1 may be sufficient to overcome the lack of AtFLIP4-2 when AtFLIP4-2 is not present in the knock-out mutants and vice versa. Ideally, double knock-out plants would then be used; however, multiple attempts to identify AtFLIP4-1 and AtFLIP4-2 double knock-outs after crosses have failed, suggest that complete lack of AtFLIP4 protein is lethal. A possible solution is to cross AtFLIP4-2 knock-out mutant plants

with heterozygous AtFLIP4-1 mutant plants and infect these plants with transformed *A. tumefaciens* containing the TAP-tag/FLIP4-2. AtFLIP4-2 complementation plants from the next generation (T_2) could then be used.

Concluding Remarks

The main objective of this study was to develop a TAP protocol for identifying protein-protein binding partners for Matrix Attachment Region-Binding Filament-Like Protein 1 (AtMFP1) and Filament-Like Protein 4-2 (AtFLIP4-2). MFP1/cTAPi and FLIP4-2/cTAPi were cloned and successfully transformed into *A. tumefaciens* GV3101 through electroporation and confirmed through colony PCR. This work has provided the basis for a continuing project.

Other research avenues were explored during this project to further investigate the potential function of AtFLIP4-1 and AtFLIP4-2. These avenues included the utilization of a large-scale yeast two-hybrid analysis which provided candidate interaction partners for AtFLIP4-2 and AtFLIP4-1. A bioinformatics study of the associated potential binding partners for AtFLIP4-2 was performed and a protein interaction map was created for AtFLIP4-1 and AtFLIP4-2. A selection of cDNA clones of these potential binding partners for AtFLIP4-1 and AtFLIP4-2 were cloned into the Gateway entry vector. This work has provided clues for further understanding of the AtFLIP4 gene family and starting material for future research. Through testing of yeast two-hybrid analysis this study confirmed AtFLIP4-2 interaction with RanGAP, and the presence of an activation domain in AtFLIP4-2.

Plant coiled-coil proteins are known to be involved in the organizational and structural roles of the plant cells along with protein-protein interactions (Rose and

Meier 2004). The evidence identified in this thesis points to new future research avenues to further investigate the functions for these unique plant-specific coiled-coil proteins.

Literature Cited

Ahlfors R, Lång S, Overmyer K, Jaspers P, Brosché M, Tauriainen A, Kollist H, Tuominen H, Belles-Boix E, Piippo M, Inzé D, Palva ET, Kangasjärvi, J. 2004. Arabidopsis RADICAL-INDUCED CELL DEATH1 belongs to the WWE protein-protein interaction domain protein family and modulates abscisic acid, ethylene, and methyl jasmonate responses. Plant Cell. 16(7):1925-1937.

Andrès C, Agne B, Kessler F. 2011. Preparation of multiprotein complexes from Arabidopsis chloroplasts using tandem affinity purification. Method Mol Biol. 775:31-49.

Arabidopsis Interactome Mapping Consortium. 2011. Evidence for network evolution in an Arabidopsis interactome map. Science. 333(6042):601-607.

Barker MS, Vogel H, Schranz ME. 2009. Paleopolyploidy in the Brassicales: analyses of the *Cleome* transcriptome elucidate the history of genome duplications in *Arabidopsis* and other Brassicales. Genome Biol Evol. 1:391-399.

Berggård T, Linse S, James P. 2007. Methods for the detection and analysis of protein-protein interactions. Proteomics. 7(16):2833-2842.

Bracha-Drori K, Shichrur K, Katz A, Oliva M, Angelovici R, Yalovsky S, Ohad N. 2004. Detection of protein-protein interactions in plants using bimolecular fluorescence complementation. Plant J. 40(3):419-427.

Bubeck J, Scheuring D, Hummel E, Langhans M, Viotti C, Foresti O, Denecke J, Banfield DK, Robinson DG. 2008. The syntaxins SYP31 and SYP81 control ER-Golgi trafficking in the plant secretory pathway. Traffic. 9(10):1629-1652.

Burkhard P, Stetefeld J, Strelkov SV. 2001. Coiled coils: a highly versatile protein folding motif. Trends Cell Biol. 11(2):82-88.

Cavalier-Smith T. 2000. Membrane heredity and early chloroplast evolution. Trends Plant Sci. 5(4):171-182.

Cole MA. 2014. Characterization of the promoter regions of FLIP4-1 and FLIP4-2 in *Arabidopsis thaliana* [honors thesis]. Appalachian State University.

Crick FHC. 1953. The packing of α-helices: simple coiled-coils. Acta Crystallogr. 6:689-697.

Criekinge WV, Beyaert R. 1999. Yeast two-hybrid: State of the Art. Biol Proced Online. 2:1-38.

Curtis SE, Clegg MT. 1984. Molecular evolution of chloroplast DNA sequences. Mol Biol Evol. 1(4):291-301.

Davis AM, Hall A, Millar AJ, Darrah C, Davis SJ. 2009. Protocol: streamlined sub-protocols for floral-dip transformation and selection of transformants in *Arabidopsis thaliana.* Plant Methods. 5:3.

Ferro M, Salvi D, Brugière S, Miras S, Kowalski S, Louwagie M, Garin J, Joyard J, Rolland N. 2003. Proteomics of the chloroplast envelope membranes from *Arabidopsis thaliana*. Mol Cell Proteomics. 2(5):325-345.

Fields S, Song O. 1989. A novel genetic system to detect protein-protein interactions. Nature. 340(6230):245-246.

Flagel LE, Wendel JF. 2009. Gene duplication and evolutionary novelty in plants. New Phytol. 183(3):557-564.

Gindullis F, Meier I. 1999. Matrix attachment region binding protein MFP1 is localized in discrete domains at the nuclear envelope. Plant Cell. 11(6):1117-1128.

Gindullis F, Peffer NJ, Meier I. 1999. MAF1, a novel plant protein interacting with matrix attachment region binding protein MFP1, is located at the nuclear envelope. Plant Cell. 11(9):1755-1768.

Havighorst A. 2012. Analysis of the function of Matrix Attachment Region-Binding Filament-Like Protein 1 (MFP1) in the chloroplast thylakoid membrane of *Arabidopsis thaliana* [master's thesis]. Appalachian State University.

Jackrel ME, Cortajarena AL, Liu TY, Regan L. 2010. Screening libraries to identify proteins with desired binding activities using a split-GFP reassembly assay. ACS Chem Biol. 5(6):553-562.

James P, Halladay J, Craig EA. 1996. Genomic libraries and a host strain designed for highly efficient two-hybrid selection in yeast. Genetics. 144(4): 1425-1436.

Jeong SY, Rose A, Meier I. 2003. MFP1 is a thylakoid-associated, nucleoid-binding protein with a coiled-coil structure. Nucleic Acids Res. 31(17):5175-5185.

Judge MT. 2015. Evidence for subfunctionalization of the FLIP4 gene family in *Arabidopsis thaliana* [honors thesis]. Appalachian State University.

Kammerer RA. 1997. Alpha-helical coiled-coil oligomerization domains in extracellular proteins. Matrix Biol. 15(8-9):555-565.

Kobayashi T, Takahara M, Miyagishima S, Kuroiwa H, Sasaki N, Ohta N, Matsuzaki M, Kuroiwa T. 2002. Detection and localization of a chloroplast-encoded HU-like protein that organizes chloroplast nucleoids. Plant Cell. 14(7):1579-1589.

Kroll D, Meierhoff K, Bechtold N, Kinoshita M, Westphal S, Vothknecht UC, Soll J, Westhoff P. 2001. VIPP1, a nuclear gene of *Arabidopsis thaliana* essential for thylakoid membrane formation. Proc Natl Acad Sci USA. 98(7):4238–4242.

Lie J W, Rose RJ. 1992. The spinach chloroplast chromosome is bound to the thylakoid membrane in the region of the inverted repeat. Biochem Biophys Res Commun. 184(2):993-1000.

Litowski JR, Hodges RS. 2001. Designing heterodimeric two-stranded alpha-helical coiled-coils: the effect of chain length on protein folding, stability and specificity. J Pept Res. 58(6):477-492.

Lupas A. 1997. Prediction coiled-coil regions in proteins. Curr Opin Struct Biol. 7(3):388-393.

Magliery TJ, Wilson CG, Pan W, Mishler D, Ghosh I, Hamilton AD, Regan L. 2004. Detecting protein-protein interactions with a green fluorescent protein fragment reassembly trap: scope and mechanism. J Am Chem Soc. 127(1):146-157.

Margulis L. 1981. The inheritance of acquired microbes. Symbiosis in cell evolution. San Francisco (CA): W. H. Freeman. p. 340.

Mason JM, Arndt KM. 2004. Coiled coil domains: stability, specificity, and biological implications. Chembiochem. 5(2):170-176.

Meier I, Zhou X, Brkljacić J, Rose A, Zhao Q, Xu XM. 2010. Targeting proteins to the plant nuclear envelope. Biochem Soc Trans. 38(3):733-740.

Monson RK. 2003. Gene duplication, neofunctionalization, and the evolution of C4 photosynthesis. Int J Plant Sci. 164(S3):S43-S54.

Mukhtar MS, Carvunis AR, Dreze M, Epple P, Steinbrenner J, Moore J, Tasan M, Galli M, Hao T, Nishimura MT, Pevzner SJ, Donovan SE, Ghamsari L, Santhanam B, Romero V, Poulin MM, Gebreab F, Gutierrez BJ, Tam S, Monachello D, Boxem M, Harbort CJ, McDonald N, Gai L, Chen H, He Y; European Union Effectoromics Consortium, Vandenhaute J, Roth FP, Hill DE, Ecker JR, Vidal M, Beynon J, Braun P, Dangl JL. 2011. Independently evolved virulence effectors converge onto hubs in a plant immune system network. Science. 333(6042):596-601.

Odgren PR, Harvie LW Jr, Fey EG. 1996. Phylogenetic occurrence of coiled coil proteins: implications for tissue structure in metazoa via a coiled coil tissue matrix. Proteins. 24(4):467-484.

Patel S, Brkljacic J, Gindullis F, Rose A, Meier I. 2005. The plant nuclear envelope protein MAF1 has an additional location at the Golgi and binds to a novel Golgi-associated coiled-coil protein. Planta. 222(6):1028-1040.

Reel KB. 2013. Redundancy and specialization in the *Arabidopsis thaliana* FLIP4 gene family [honors thesis]. Appalachian State University.

Richardson CA. 2012. Localization of FLIP4-2 via immunofluorescence microscopy in *Arabidopsis thaliana* leaf cross sections [honors thesis]. Appalachian State University.

Robinson C, Thompson SJ, Woolhead C. 2001. Multiple pathways used for the targeting of thylakoid proteins in chloroplasts. Traffic. 2(4):245-251.

Rohila J, Chen M, Cerny R, Fromm ME. 2004. Improved tandem affinity purification tag and methods for isolation of protein heterocomplexes from plants. Plant J. 38:172-181.

Rose A, Manikantan S, Schraegle SJ, Maloy MA, Stahlberg EA, Meier I. 2004. Genome-wide identification of Arabidopsis coiled-coil proteins and establishment of the ARABI-COIL database. Plant Physiol. 134(3):927-939.

Rose A, Meier I. 2004. Scaffold, levers, rods and springs: diverse cellular functions of long coiled-coil proteins. Cell Mol Life Sci. 61(16):1996-2009.

Rose A, Schraegle SJ, Stahlberg EA, Meier I. 2005. Coiled-coil protein composition of 22 proteomes- differences and common themes in subcellular infrastructure and traffic control. BMC Evol Biol. 5:66.

Samaniego R, de la Torre C, Moreno Díaz de la Espina S. 2008. Characterization, expression and subcellular distribution of a novel MFP1 (matrix attachment region-binding filament-like protein 1) in onion. Protoplasma. 223(1-2):31-38.

Samaniego R, Yu W, Meier I, Moreno Díaz de la Espina S. 2001. Characterization and high-resolution distribution of a matrix attachment region-binding protein (MFP1) in proliferating cells of onion. Planta. 212:535-546.

Sato N, Ohshima K, Watanabe A, Ohta N, Nishiyama Y, Joyard J, Douce R. (1998). Molecular characterization of the PEND protein, a novel bZIP protein present in the envelope membrane that is the site of nucleoid replication in developing plastids. Plant Cell. 10:859-872.

Sato N, Rolland N, Block MA, Joyard J. 1999. Do plastid envelope membrans play a role in the expression of the plastid genome? Biochimie. 81: 619-629.

The Arabidopsis Genome Initiative. 2000. Analysis of the genome sequence of the flowering plant *Arabidopsis thaliana*. Nature. 408(6814):796-815.

Waese J, Fan J, Pasha A, Yu H, Fucile G, Shi R, Cumming M, Kelley L, Sternberg M, Krishnakumar V, Ferlanti E, Miller J, Town C, Stuerzlinger W, Provart NJ. 2017. ePlant: visualizing and exploring multiple levels of data for hypothesis generation in plant biology. Plant Cell. 29(8):1806-1821.

Xu X, Song Y, Li Y, Chang J, Zhang H, An L. 2010. The tandem affinity purification method: an efficient system for protein complex purification and protein interaction identification. Protein Expr Purif. 72(2):149-156.

Vita

Alison Ruth DeShields was born in 1983 to Kathy Steinbeck in Pensacola, Florida. She entered the University of West Florida to study biology and art, and in December 2006 was awarded the Bachelor of Science degree with a minor in Studio Art. She was accepted into Appalachian State University in pursuit of a Master's degree in Cell and Molecular Biology, where she worked in the laboratory of Dr. Annkatrin Rose and received her Master of Science in December 2017.